WHIRLWIND PROGRAMMING OF S_2 APPROXIMATION FOR FLUX DISTRIBUTION IN A FINITE CYLINDRICAL REACTOR

William Edward Campbell, Jr.
and
Vincent William Panciera

Cambridge 39, Massachusetts
27 May 1957

Secretary of the Faculty
Massachusetts Institute of Technology
Cambridge 39, Massachusetts

Dear Sir:

We hereby submit our thesis, Whirlwind Programming of S_2 Approximation for Flux Distribution in a Finite Cylindrical Reactor, in partial fulfillment for the degree of Naval Engineer and the degree of Master of Science in Naval Architecture and Marine Engineering.

Whirlwind Programming of S_2 Approximation for Flux Distribution in a Finite Cylindrical Reactor

by

William Edward Campbell, Jr., Lieutenant, U. S. Navy
B.S., U. S. Naval Academy, 1951

and

Vincent William Panciera, Lieutenant, U. S. Navy
B.S., U. S. Naval Academy, 1951

submitted in partial fulfillment of the requirements for the degree of
Naval Engineer
and the degree of
Master of Science in Naval Architecture and Marine Engineering

at the
Massachusetts Institute of Technology

June 1957

Thesis
C194

Whirlwind Programming of S_2 Approximation for Flux Distribution in a Finite Cylindrical Reactor

by

William E. Campbell Jr.
Lieutenant, U.S. Navy

Vincent W. Panciera
Lieutenant, U.S. Navy

Submitted to the Department of Naval Architecture and Marine Engineering on May 27, 1957 in partial fulfillment of the requirements for the degree of Naval Engineer and the degree of Master of Science in Naval Architecture and Marine Engineering.

ABSTRACT

This thesis attempts to develop a program for the Whirlwind computer operating in the interpretive mode for the flux distribution in a finite cylindrical reactor.

The reactor chosen for investigation was a hypothetical organic moderated, highly enriched, cylindrical reactor having a power output capable of fulfilling one half the propulsive requirements of a nuclear powered naval cruiser.

Heat transfer and basic physics calculations were accomplished to determine preliminary size and material requirement of such a reactor.

The flux equations were derived using numerical integration methods suitable for computer programming.

35734

Conclusion

1) The code as presently programmed is incorrect.
2) The grid spacing as used is much too coarse. This difficulty is not inherent in the coded program.
3) The mode of computer operation is unsuitable for an iterative process such as this because it results in a code that progresses too slowly.

Recommendations

1) Prior to the use of any computer a formal or semi-formal course in programming should be completed.
2) A grid spacing comparable to the mean free path of the neutron should be selected.
3) The fastest possible mode of calculation on the computer available should be used.
4) For a coded program of this difficulty a faster machine with a much larger fast memory is very desirable.

Thesis Supervisor — Melville Clark, Jr.

Title — Assistant Professor of Nuclear Engineering

ACKNOWLEDGEMENTS

The authors wish to express their gratitude to Professor Melville Clark, Jr., for his supervision and helpful suggestions in completing this thesis and to Mr. Marius Troost for his untiring assistance in developing the program for Whirlwind.

Table of Contents

	Page
Title Page	
Abstract	i
Acknowledgements	iii
Table of Contents	iv
I Introduction	1
II Procedure	6
A. Heat Transfer	6
B. Basic Reactor Physics	24
C. Flux Equations	27
D. Computer	37
1. Introduction	37
2. Logic	44
III Results	58
IV Discussion of Results	59
V Conclusions	61
VI Recommendations	62
VII Appendices	
A. Development of Equations Using S_2 Approximation to the Boltzmann Equation for Cylindrical Geometry	63
B. Whirlwind Program	87
C. Bibliography	99

INTRODUCTION

The desirability of a uniform power distribution $(P_{max}/P_{av}) = 1$ has long been realized since it will not only decrease the mass of the fuel required for the attainment of criticality but also will increase the total power output by allowing the whole core instead of only a small fraction of the reactor to operate at the highest allowable temperature. Operation at the highest possible temperature allowed by metallurgical considerations over the entire reactor will increase the average core life since more uniform burn up is attained.

It is possible to achieve this uniform power distribution by various means. One of the first methods to be used was that of poisons. In this method long lasting poisons are placed in the reactor structure in the anticipated locations of high flux. By placing poison in these regions the peak flux is reduced to such a level that the power density is approximately uniform. This procedure is a very wasteful one from the point of view of neutron economy. The regions of the reactor that are contributing greatly to the overall neutron efficiency of the reactor are penalized to the extent that they can be no more efficient than the most inefficient region. For power producing reactors, particularly mobile ones, this waste of neutrons is very undesirable.

The use of poison is the first of two methods that exploit a nonuniform macroscopic cross section to achieve the uniform distribution of power. The second consists in the use of a nonuniform macroscopic fission cross section. This method allows each region of

the reactor to operate most efficiently. The efficiency is determined by the position of the region within the reactor. The leakage from a reactor causes a reduction in the value of the flux at large distances from the center of the core. To compensate for this reduction in flux the macroscopic fission cross section is increased in the regions far from the center and decreased in the central portions. To this end, the fuel concentration is increased near the edges.

Neutron economy can also be improved by surrounding the core with neutron reflector material. A light substance having a relatively low absorption cross section performs this function very well, i.e., heavy water or beryllium.

Since the reactor to be investigated is intended for a hypothetical naval cruiser, the use of poisons to achieve a uniform power distribution is not desirable, for a compact reactor is required. Though the reactor must be compact, it is desirable to install a reasonably thick reflector for the purpose of improving the neutron economy, attenuating the neutrons leaking out, and cooling of the reactor shell and pressure vessel.

It would be possible to have a nonuniform macroscopic cross section of the reactor in each of its directions. For the spherical reactor the variation would be radial only, but the application of a spherical reactor to shipboard use is impractical. The normal configuration of spaces aboard a ship is rectangular and a spherical reactor does not adapt very well to this arrangement. However, a rectangular reactor allows efficient utilization of space aboard a ship, but from the nuclear point of view this shape is not too desir-

able because leakage depends on the relationship of surface area to volume. It can be seen that the neutron economy decreases in progression from the sphere to the cylinder to the rectangular parallepiped.

With these considerations in mind a right cylindrical reactor shape will be investigated. With this shape it would be possible to vary the properties in two directions, radially and axially. While this goal is theoretically interesting, it is prohibited when cost is considered. The reactor that is to be investigated will have a uniform composition in the axial direction with finite radial segments differing in properties.

For the shipboard use of a nuclear reactor power plant it is desirable to have a plant as light and safe as can possibly be designed within the space allowed but still without incorporating undue quantities of the "exotic" and expensive materials or coolants. One possible solution is the use of a highly enriched reactor using a coolant that permits high operating temperatures at low pressures and does not become dangerously radioactive while passing thru the reactor core.

A coolant that has a low vapor pressure at high operating temperature will allow a system pressure which is much lower than that employed in the present day water cooled and moderated shipboard reactor installation. The use of such a coolant will not only result in much better steam conditions, but it will also make possible an overall weight reduction, since a low pressure system can be used. The saving in weight is particularly significant in the pressure

vessel.

If the coolant does not become radioactive in its passage thru the reactor core, the shielding can be concentrated primarily around the reactor proper, provided that impurities in the coolant are kept at a very low concentration. Even with a small amount of impurities, the radiation emitted by the coolant would be low enough to permit reduced thicknesses of shielding around the primary loop.

A liquid organic hydrocarbon will fulfill the requirements listed above, but also will present some unsolved problems. It will (1) tend to increase the size of the reactor by decreasing the hydrogen moderation relative to a water cooled and moderated reactor, (2) tend to increase the reactor size due to its less efficient heat transfer capabilities compared with water and (3) exhibit both thermal and radiolytic breakdown in which the original hydrocarbon will, primarily by polymerization, change into longer chain hydrocarbons with the evolution of relatively large amounts of gas and a great increase in viscosity of the coolant.

The latter problems will be investigated at the National Reactor Testing Station on the Organic-Moderated Reactor Experiment (ORME). This experiment is not a prototype for an organic power reactor but is being built to test the feasibility of its use as a reactor coolant. [1] At the West Milton Annex of the Knolls Atomic Power Laboratory the Atomic Energy Commission plans to investigate the feasibility of an organic moderated and cooled reactor for naval propulsion. This will be conducted on the Naval Organic Reactor Experiment, (NORE).

The heat transfer properties of the various liquid organic hydrocarbons that are presently under consideration are not generally available. Some presently under investigation are diphenyl, O-terphenyl, M-terphenyl and P-terphenyl. A proprietary heat transfer medium "Dowtherm" is available commercially and is composed of 73.5% diphenyl oxide and 26.5% diphenyl. It has a working range of 450-750°F. at pressures less than 145 psig. Since "Dowtherm" closely resembles the hydrocarbons that will be investigated on the ORME and its heat transfer properties are readily available[2] it will be used in this investigation.

The fuel element chosen for this investigation is of the MTR (Materials Testing Reactor) type.[3] An effective length of element was set at 48". This length was chosen so that the overall height of the reactor, control devices and shield would fit into the present day engineering spaces of a cruiser. Any additional height would have an adverse effect on stability, since it would result in a higher shield deck and thus an increase in the height of the center of gravity of the ship.

Fuel Element Dimensions

$t_m = 0.020"$

$t_c = 0.015"$

$W = 2.5"$

$L = 48.0"$

$t_s^1 = 0.115"$ (Case 1)

$t_s^2 = 0.0919" = 0.8\ t_s^1$ (Case 2)

$t_s^3 = 0.069" = 0.6\ t_s^1$ (Case 3)

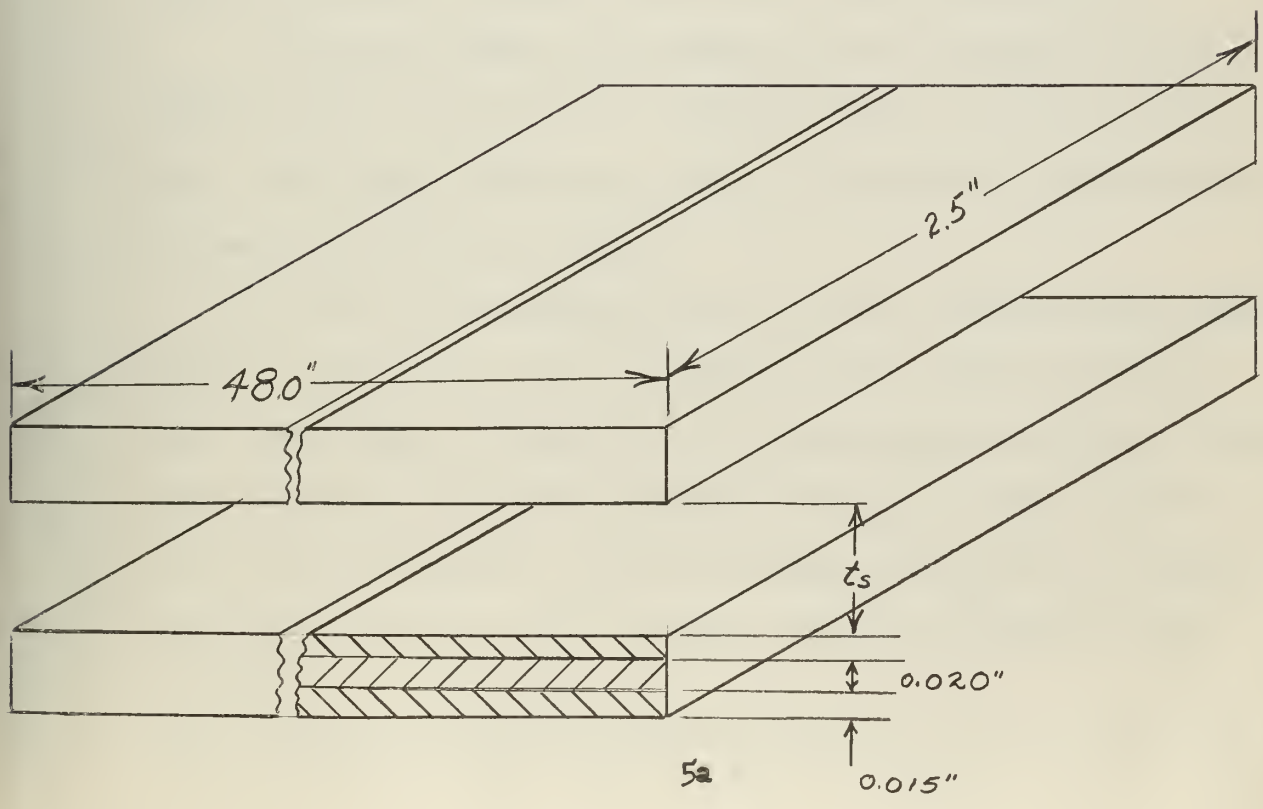

PROCEDURE

Heat Transfer[1]

The controlling variables in this study were (1) the maximum surface temperature of the fuel element or the maximum temperature at the centerline of the fuel element and (2) the maximum coolant speed. The maximum surface temperature of the fuel element may be controlling, since the preliminary investigations on the ORME have shown that above 800° F the thermal breakdown is increased greatly.[4] However, liquid loading requirements of a naval vessel make storage of used coolant a simple matter and in the interest of higher efficiency some breakdown will be accepted. Therefore, a fuel element surface temperature less than 850° F will be accepted. If the maximum fuel temperature at the centerline is allowed to exceed a value of about 1130° F, a phase transformation of uranium is encountered in which an anisotropic expansion and possible rupture of the fuel element may result. Therefore, a second design criterion will be required that the fuel element centerline temperature be less than 1130° F.

Preliminary studies on the ORME have also shown that coolant speeds greater than 15 feet per second result in excessive erosion. As a third design criterion, it will be required that coolant speed be less than 15 feet per second.

The first investigation was with a reactor coolant outlet temperature of 750° F with various temperature rises across the reactor. This investigation was amplified by varying coolant speed while holding the temperature rise across the reactor constant. Each of these situations were further studied by considering the MTR fuel element modified to the extent that the plate spacing was narrowed to 80% and 60%.

---

[1] Nomenclature for Heat Transfer on pages 22 and 23.

Though it was known in advance that the speed would be kept at or less than 15 feet per second calculations were pursued with higher values. This was done to show that a reduction in size can be accomplished in the future, if the erosion problem at high coolant speeds can be overcome.

A heat rate requirement of 6.06×10^8 Btu/hr was chosen based on the full power steaming rate of a typical cruiser.

With this value of Q (6.06×10^8) a coolant outlet temperature, coolant temperature rise, coolant speed and plate spacing are chosen. Since the inlet and outlet temperatures are known the average values of density and specific heat may be calculated. Formulae 1, 2, 3, and 4 are used respectively to calculate w, A_f, G and n.

$$w = \frac{Q}{\bar{C}_p \Delta T} = G A_f \tag{1}$$

$$A_f = \frac{w}{3600 \bar{\rho} v} \tag{2}$$

$$G = v\bar{\rho} = \frac{w}{3600 A_f} \tag{3}$$

$$n = \frac{A_f}{A_f^n} \tag{4}$$

Since the dimensions of the fuel element for each case are known, both the hydraulic diameter and the total flow area can be calculated. With the product of the mass flow rate and the hydraulic diameter the produce of the heat transfer coefficient and the hydraulic diameter can be read from the graph in the "Dowtherm" booklet. Formulae 5, 6, 7,

and 8 are then used to calculate, respectively, Q_v, ΔT_{fuel}, ΔT_{clad}, and θ.

$$Q_v = \frac{Q}{V_f} \tag{5}$$

$$\Delta T_{fuel} = T_o - T_1 = \frac{t_m^2 Q_v}{4k_f} \tag{6}$$

$$\Delta T_{clad} = T_o - T_2 = \frac{t_m Q_v t_c}{2k_c} \tag{7}$$

$$\theta = T_2 - T_b = \frac{Q_v t_m}{2h} \tag{8}$$

Datum from the calculation of a coolant outlet temperature of 750° F for various values of temperature rise and speed for cases 1, 2 and 3 are in Tables I, II, and III and Figures I, II, and III respectively. The cladding temperature existing for each of these conditions is plotted on Figure IV.

The narrowest plate spacing, case 3, gives a significantly smaller reactor. Since the pumping power of any of these cases proved to be very small compared with the total power output, it was decided to investigate the result of a decrease of coolant outlet temperature for this case only. Coolant outlet temperature was reduced to 700° V and the speed was held at 15 feet per second. Datum from this calculation are in Table IV. These data were plotted as a dotted line on Figure IV.

For these twelve conditions the fraction of uranium in the uranium-zirconium dispersed fuel plate was calculated and plotted on Figure V. It is desirable that the fuel be of such a composition that it contributes

TABLE I

Datum for coolant outlet of 750° F
and wide plate spacing
(case 1)

A. REACTOR ΔT = 200°F

v (ft/sec)	G ($lb/sec-ft^2$)	h ($Btu/hr-ft^2-°F$)	A_f (ft^2)	n (no. of plates)
5	236.1	686.	5.36	2,685
15	709.0	1611.	1.79	896
25	1180.0	2340.	1.07	538
50	2360.0	4090.	0.54	269

v (ft/sec)	$Q_v \times 10^8$ ($Btu/hr-ft^3$)	T_o-T_1 (°F)	T_1-T_2 (°F)	T_2-T_b (°F)	T_2 (°F)	f_u %
15	4.86	20.7	62.2	215.8	1015.8*	25.4

B. REACTOR ΔT = 150°F

v (ft/sec)	G ($lb/sec-ft^2$)	h ($Btu/hr-ft^2-°F$)	A_f (ft^2)	n (no. of plates)
5	231.9	682.	7.26	3,639
15	705.0	1591.	2.42	1,211
25	1160.0	2320.	1.45	727
50	2318.0	4040.	0.73	364

v (ft/sec)	$Q_v \times 10^8$ ($Btu/hr-ft^3$)	T_o-T_1 (°F)	T_1-T_2 (°F)	T_2-T_b (°F)	T_2 (°F)	f_u %
15	3.60	15.4	46.0	197.3	947.3*	19.5

---

*excessive temperature

γuranium content too low

Table I (Continued)

C. REACTOR ΔT = 100°F

v (ft/sec)	G (lb/sec-ft^2)	h (Btu/hr-ft^2-°F)	A_f (ft^2)	n (no. of plates)
5	227.	669.	11.01	5,520
15	681.	1569.	3.67	1,839
25	1135.	2295.	2.02	1,103
50	2270	4000.	1.10	552

v (ft/sec)	$Q_v \times 10^8$ (Btu/hr-ft^3)	T_o-T_1 (°F)	T_1-T_2 (°F)	T_2-T_b (°F)	T_2 (°F)	f_u %
15	2.37	10.1	30.3	133.8	883.8*	13.5

D. REACTOR ΔT = 50°F

v (ft/sec)	G (lb/sec-ft^2)	h (Btu/hr-ft^2-°F)	A_f (ft^2)	n (no. of plates)
5	221.8	659.	22.40	11,230
15	667.0	1545.	7.45	3,730
25	1110.0	2275.	4.47	2,240
50	2218.0	3910.	2.24	1,123

v (ft/sec)	$Q_v \times 10^8$ (Btu/hr-ft^3)	T_o-T_1 (°F)	T_1-T_2 (°F)	T_2-T_b (°F)	T_2 (°F)	f_u %
15	1.17	4.97	15.0	66.2	816.2	6.99

---

* excessive temperature

† uranium content too low

TABLE II

Datum for coolant outlet of 750°F,
coolant speed of 15 ft/sec, and medium plate spacing
(case 2)

ΔT (°F)	G ($lb/sec-ft^2$)	h ($Btu/hr-ft^2-°F$)	n (no. of plates)	$Q_v \times 10^8$ ($Btu/hr-ft^3$)
200.	709.	1671.	1121.	3.89
150.	705.	1660.	1515.	2.88
100.	681.	1639.	2300.	1.89
50.	667.	1631.	4660.	0.94

ΔT (°F)	T_o-T_1 (°F)	T_1-T_2 (°F)	T_2-T_b (°F)	T_2 (°F)	f_u %
200	16.6	49.7	193.9	943.9*	19.6
150	12.3	36.9	144.2	894.0*	16.1
100	8.1	24.3	96.3	846.3	11.0
50	4.0	12.0	47.6	797.6	5.6γ

*temperature excessive

γuranium content too low

TABLE III

Datum for coolant outlet of 750°F,
coolant speed of 15 ft/sec, and narrow plate spacing
(case 3)

ΔT (°F)	G (lb/sec-ft^2)	h (Btu/hr-ft^2-°F)	n (no. of plates)	$Q_v \times 10^8$ (Btu/hr-ft^3)
200	709	1796	1496	2.9
150	705	1775	2020	2.2
100	681	1731	3061	1.4
50	667	1718	6230	0.70

ΔT (°F)	$T_o - T_1$ (°F)	$T_1 - T_2$ (°F)	$T_2 - T_b$ (°F)	T_2 (°F)	f_u %
200	12.4	37.3	135.2	885.2*	16.3
150	9.2	27.6	101.3	851.3	12.4
100	6.1	18.2	68.5	818.5	8.4$^\gamma$
50	3.0	9.0	33.9	783.9	4.3$^\gamma$

*temperature excessive

$^\gamma$uranium content too low

FIGURE 7

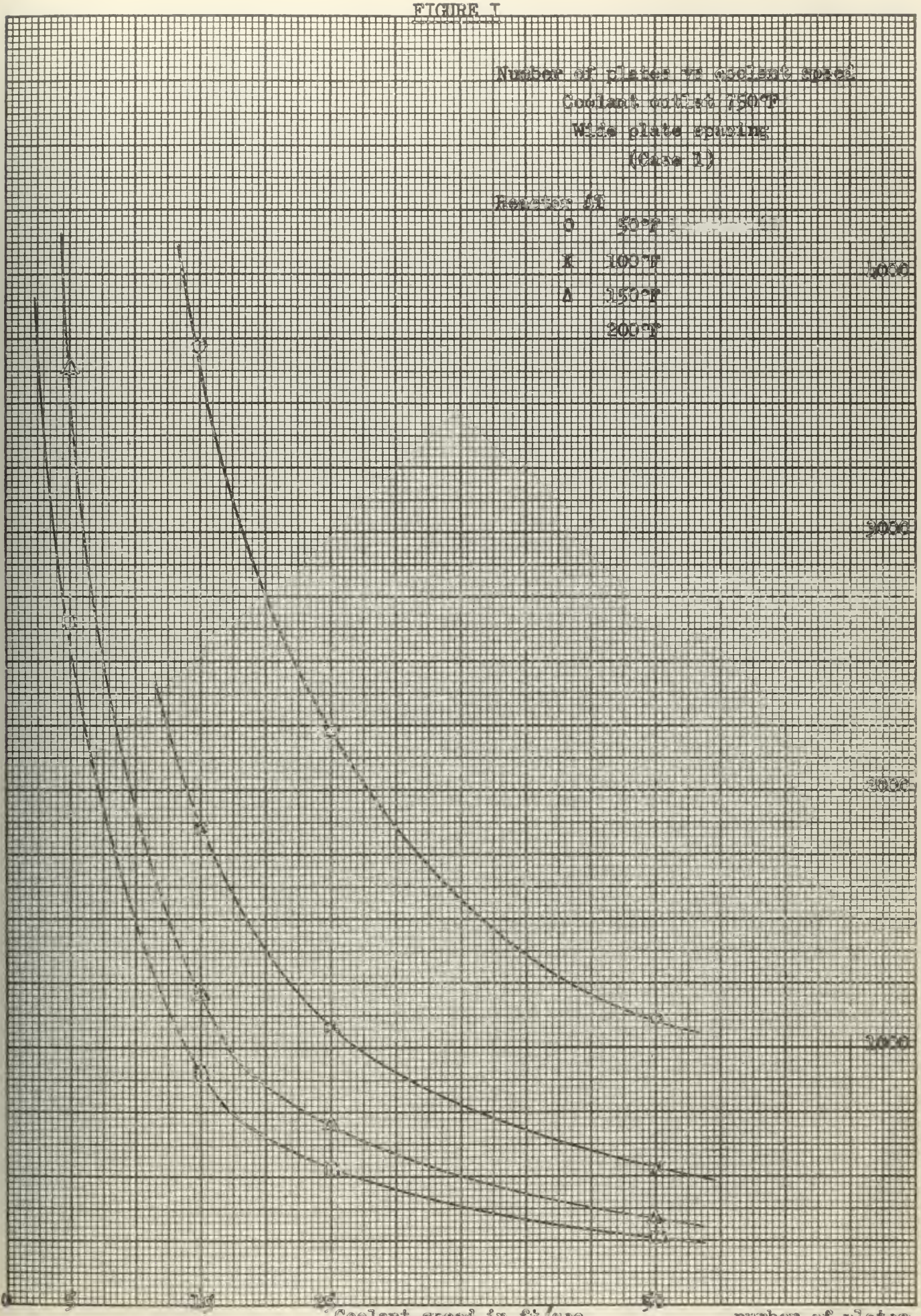
Number of plates vs coolant speed
Coolant outlet 750°F
Wide plate spacing
(Case 1)
Reactor ΔT
○ 50°F
× 100°F
Δ 150°F
200°F
4000
3000
2000
1000
0
5
10
15
20
Coolant speed in ft/sec
number of plates

FIGURE II

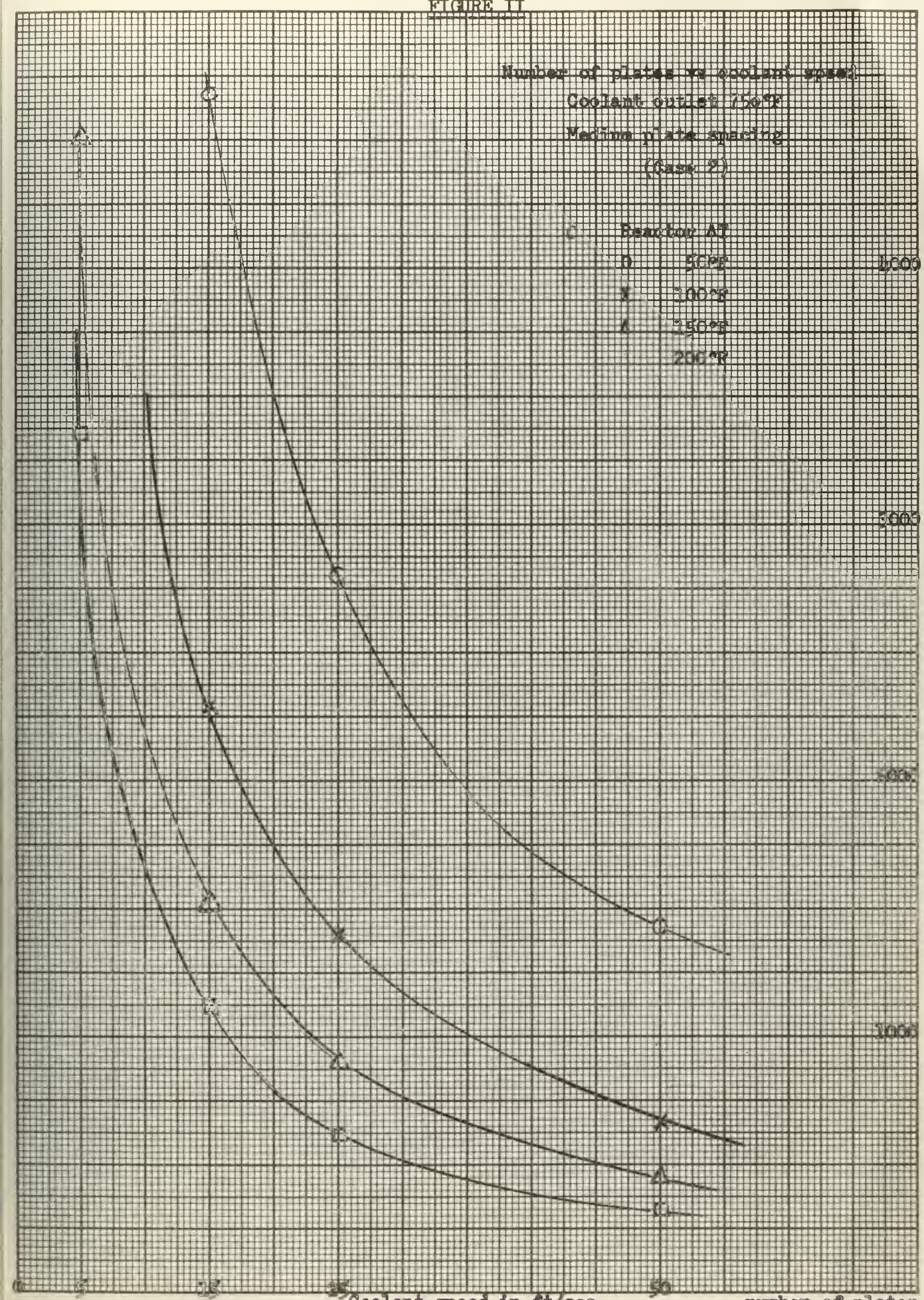
Number of plates vs coolant speed
Coolant outlet 750°F
Medium plate spacing
(Case 2)
Reactor ΔT
50°F
100°F
150°F
200°F
4000
3000
2000
1000
5
10
25
50
Coolant speed in ft/sec
number of plates

FIGURE III

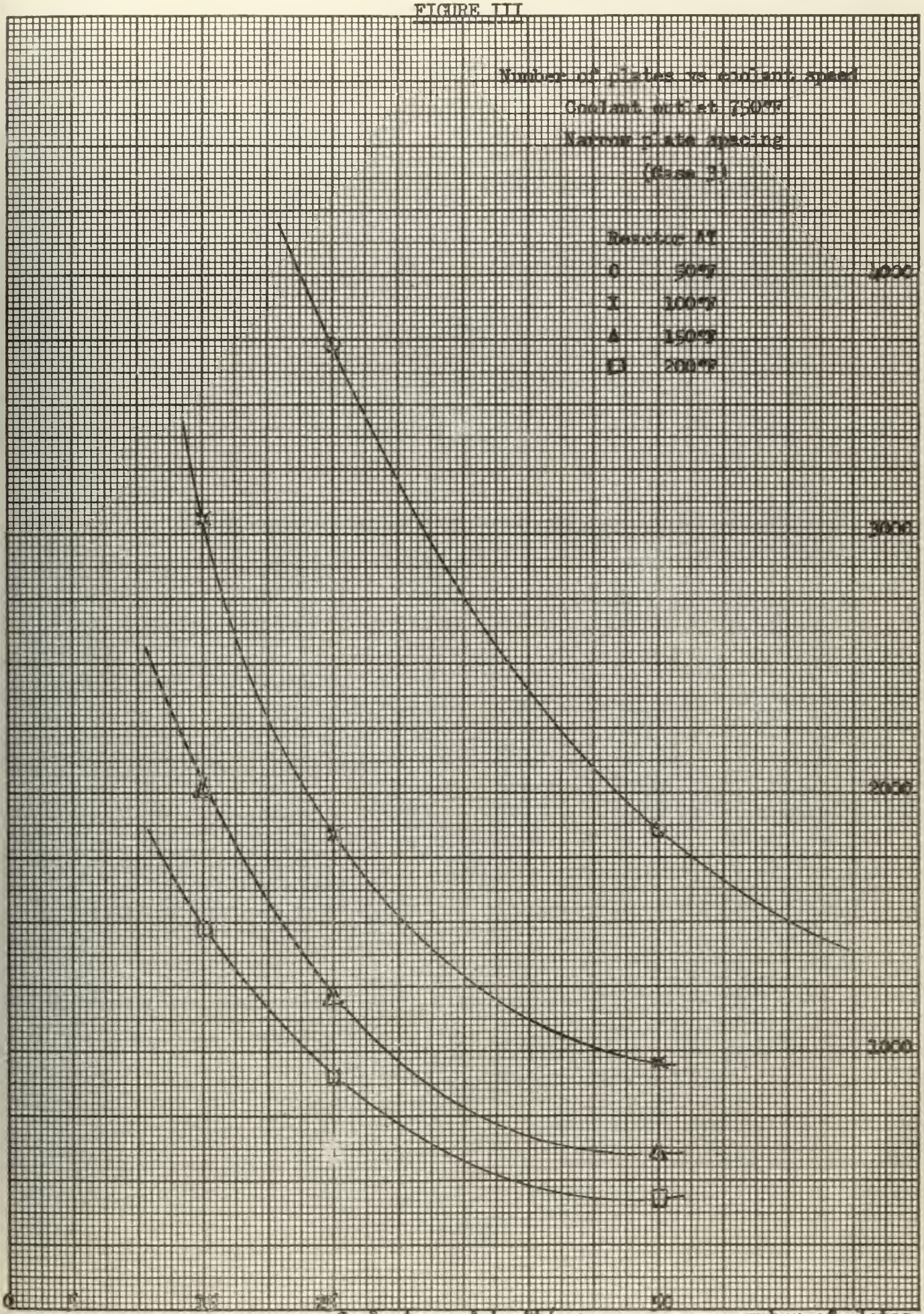
Number of plates vs coolant speed
Coolant outlet 750°F
Narrow plate spacing
(Case 3)
Reactor ΔT
C 50°F
X 100°F
A 150°F
B 200°F
4000
3000
2000
1000
0
Coolant speed in ft/sec
number of plates

TABLE IV

Datum for coolant outlet of 700°F,
coolant speed of 15 ft/sec, and narrow plate spacing
(case 3)

ΔT (°F)	G (lb/sec-ft^2)	h (Btu/hr-ft^2-°F)	n (no. of plates)	$Q_v \times 10^8$ (Btu/hr-ft^3)
200	739.5	1826	871	5.0
150	726.8	1812	1164	3.7
100	712.5	1775	1767	2.5

ΔT (°F)	$T_o - T_1$ (°F)	$T_1 - T_2$ (°F)	$T_2 - T_b$ (°F)	T_2 (°F)	f_u %
200	21.3	64.0	228.4	924.4*	26.0
150	15.9	47.9	172.2	872.2	20.3
100	10.5	31.5	115.8	815.8	14.0

---

* temperature excessive

γ uranium content too low

FIGURE IV

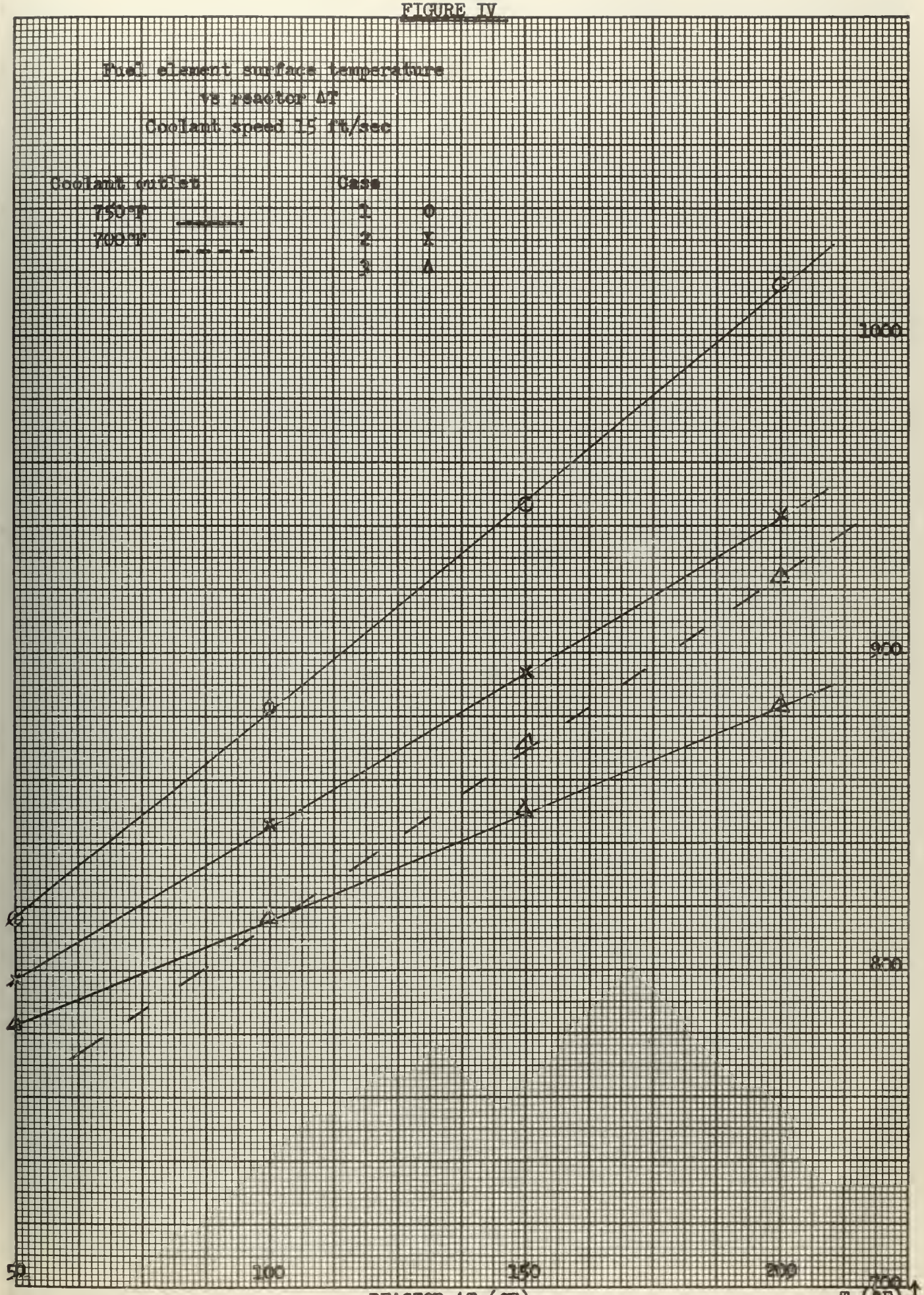
Fuel element surface temperature
vs reactor ΔT
Coolant speed 15 ft/sec
Coolant outlet
750°F
700°F
Case
1 ○
2 X
3 △
1000
900
800
50
100
150
200
250
REACTOR ΔT (°F)
T_2(°F)

FIGURE V

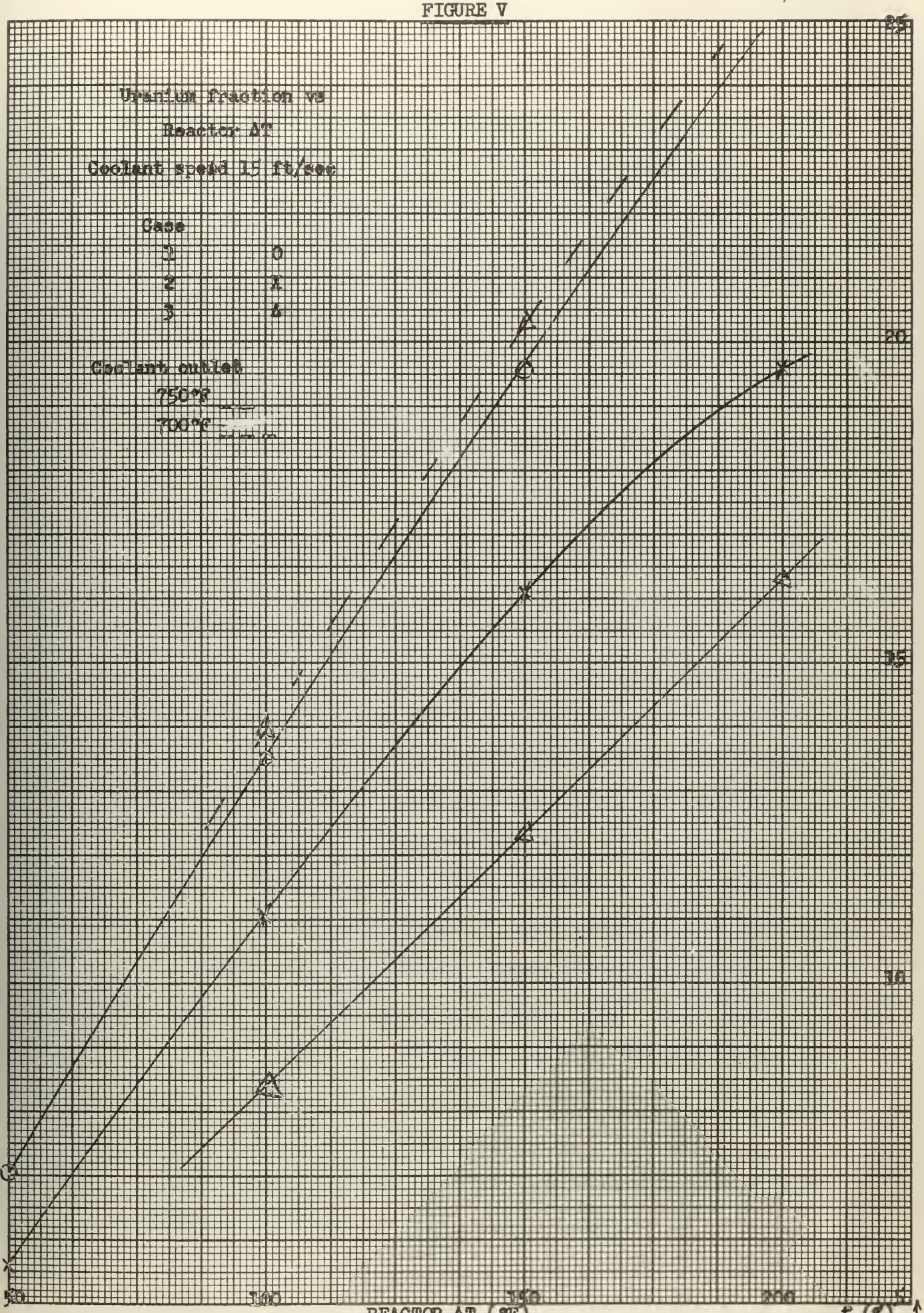
Uranium fraction vs
Reactor ΔT
Coolant speed 15 ft/sec
Case
1 0
2 X
3 Δ
Coolant outlet
750°F
700°F
25
20
15
10
50
100
150
200
REACTOR ΔT (°F)
f_u(%)

to the structural strength of the reactor. A uranium content of 10% by weight or greater has desirable strength characteristics.

Of the six conditions that have a fuel element surface temperature of less than 850° F only two have a uranium fraction of above 10%. These are shown in Table V.

t_{co}	T	case	n	T_2
750	100	3	3061	818
700	100	3	1767	815

Table V Particularly Interesting Cases

Figure VI shows the variation in number of plates for case 3 holding the coolant speed at 15 feet per second and varying the temperature rise across the reactor.

The size resulting from the condition with a coolant outlet temperature of 700° F is better for the following reasons:

1) it is by far the smaller,

2) the increase of uranium fraction by 2 1/2% gives a significant increase in the strength of the fuel region.

With this condition the fuel element surface temperature will be less than the prescribed value of 850° F. The amount of damage that will result to the coolant from this temperature and the accompanying radiation is uncertain. However, for shipboard applications it does not appear to be a serious penalty.

In the present day cruiser design for torpedo protection there is available a large amount of bunker fuel oil to partially fill the

FIGURE VI

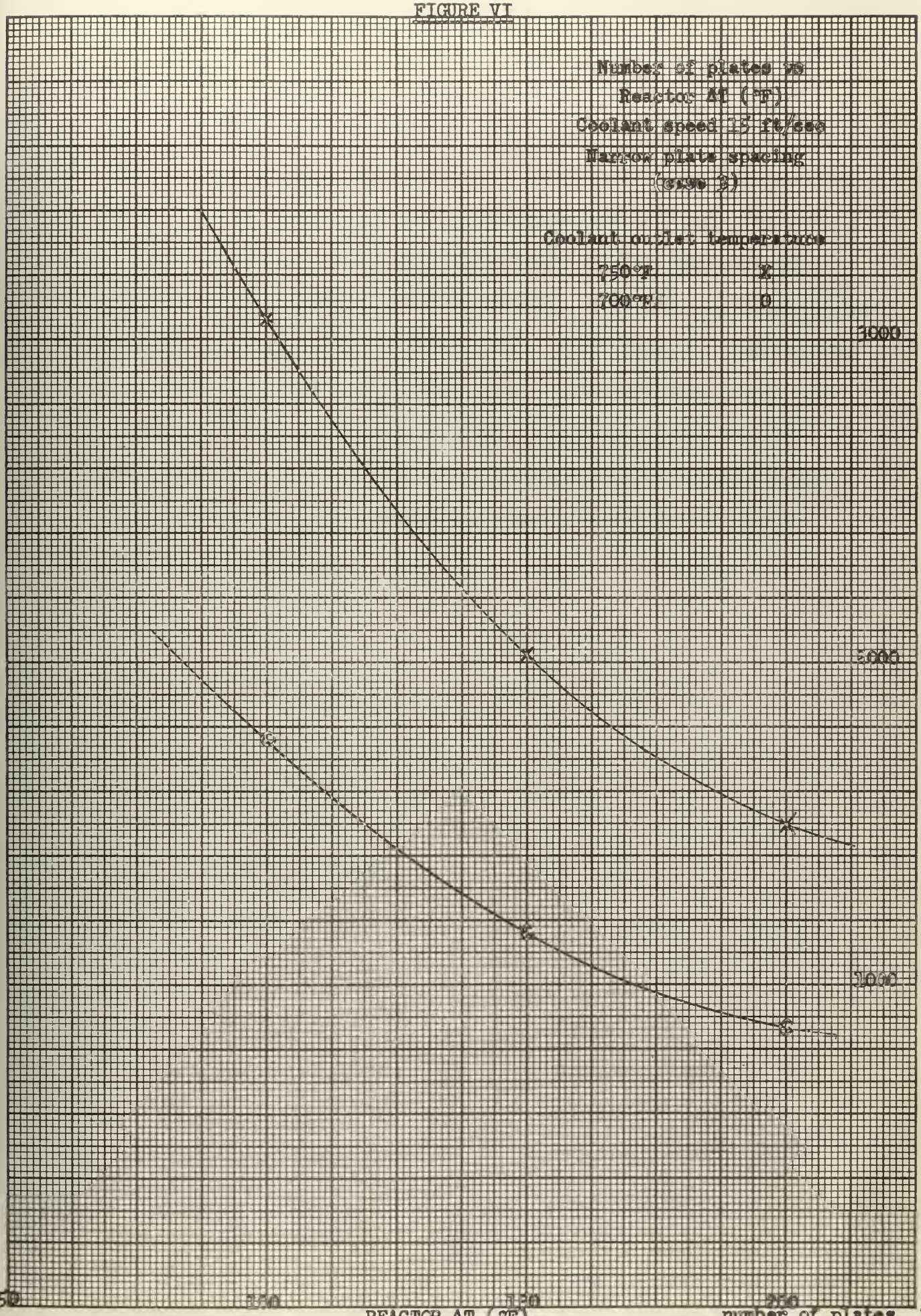
Number of plates vs
Reactor ΔT (°F)
Coolant speed 15 ft/sec
Narrow plate spacing
(Case 3)
Coolant outlet temperature
750°F X
700°F O
3000
2000
1000
50
250
500
REACTOR ΔT (°F)
number of plates

layers of the torpedo protective system. Certain layers of the torpedo protective system are required to be liquid loaded. This system could be used for the storage of the organic moderator coolant. The unradiated coolant could be stored in the inner layers of the system and that which had been irradiated would be stored in the outer layers to protect the crew from any induced radioactivity. The long chain hydrocarbons would tend to settle to the lower parts of the tanks where they could be removed during periods of overhaul. With the installation of a purification system this process of separation might be handled continuously aboard ship in the same manner that lubrication oil is purified and recycled.

Nomenclature

A_f	flow total area, (ft^2)
A_f^n	flow area per plate case n, (ft^2/plate)
A_h	heat transfer area, (ft^2/plate)
$\bar{c}_p$	average specific heat, (Btu/lb °F)
D'	hydraulic diameter, (inches)
f_u	fraction of uranium in fuel region
G	mass flux, (lb/sec-ft^2)
h	film coefficient, (Btu/hr-ft^2-°F)
k_c	thermal conductivity of cladding, (Btu/hr-ft-°F)
k_f	thermal conductivity of cladding, (Btu/hr-ft-°F)
L	fuel length, (inches)
n	number of fuel plates
Q	total heat generation rate, (Btu/ft^3)
Q_v	heat generation rate per unit volume of fuel, (Btu/hr-ft^3)
t_c	fuel cladding thickness, (inches)
t_{co}	coolant outlet temperature, (°F)
t_m	fuel thickness, (inches)
t_s	spacing between plates, (inches)
T_b	bulk temperature of coolant, (°F)

Nomenclature (Continued)

T_o	fuel centerline temperature, (°F)
T_1	fuel-clad interface temperature, (°F)
T_2	fuel element surface temperature, (°F)
U	overall heat transfer coefficient, (Btu/hr-ft^2-°F)
v	coolant speed, (ft/sec)
w	mass rate of flow, (lb/hr)
W	fuel width, (inches)
ΔT	overall temperature difference across reactor, (°F)
$\bar{\rho}$	average density, (lb/ft^3)
θ	film temperature drop, (°F)

Basic Reactor Physics

Criticality calculations were made using a one group reflected homogenous model with case 3, narrow fuel elements. Based on heat transfer considerations, inlet and outlet coolant temperature were set at 600° and 700° F, respectively, with a coolant speed of 15 ft/sec.

The assumptions in this calculation were

1. The structural members inside the reactor were of type 347 stainless steel and composed ten percent of the total reactor weight,
2. A fast fission factor of unity,
3. The uranium of fuel is enriched to 90% in U^{235},
4. A right circular, cylindrical flux distribution of a cosine axially and a Bessel function radially,
5. A beryllium reflector of 236 cm placed around the reactor.

The reactor was treated as a homogeneous medium. By a one group calculation the volumes of each constituent of the reactor were calculated from the dimensions given previously in the heat transfer section. These volumes were then converted to weights and the volume fraction of the total reactor as shown in Table I. From the cross sections given in BNL-325[5] effective cross sections were calculated for the operating temperature of the material. With these cross sections the reactor parameters as shown in Table II were calculated. These give an effective multiplication factor of 0.894. This value is sufficiently close to unity that final adjustments are made by the computing machine.

The primary purpose of the calculation is to obtain an approximate

value of the critical radius which is needed as an input to the computer solution.

Table I

Reactor Materials

	Volume (cm^3)	Mass (Kgm)	Volume fraction
Fuel	6.95×10^4	495.	
U		69.5	0.0068
Zr		425.5	0.408
Clad (Zr)	15.01×10^4	966	
Stainless Steel	1.99×10^4	160	
Cr (18% by weight)		28.4	0.007
Ni (11% by weight)		17.35	0.004
Fe (71% by weight)		112.	0.027
Coolant	26.3×10^4	219.5	
[73.5 Diphenyl oxide by weight ($C_6H_5OC_6H_5$) and 26.5% Diphenyl by weight $(C_6H_5)_2$]			
C (06.91 by weight)			0.47043
H (06.03 by weight)			0.03292
O (86.59 by weight)			0.3774

Table II

Reactor Parameters

δ = Beryllium shield thickness	=	23.6 cm.
$\Sigma_{tr} = \sum_i \Sigma_{s_i} (1-\mu_o)_i V_f \left\{ 1 - \frac{4}{5} \frac{\Sigma_{a_i}}{\Sigma_{t_i}} \right\}$	=	0.28334 cm^{-1}
$D = 3 \frac{1}{\Sigma_{t_{tr}}}$	=	1.17644 cm
$d = 0.71 \lambda_{tr} \frac{1+\beta}{1-\beta} = 33.7D$	=	39.599 cm
$\Sigma_a = \sum_i \Sigma_{a_i} V_f$	=	0.1208 cm^{-1}
$L^2 = \frac{D}{\Sigma_a}$	=	9.7387 cm^2
$p(E) = \exp \frac{\bar{N}_{28} (3.9)}{\xi \Sigma_s} \left(\frac{\Sigma_s \times 10^{24}}{\bar{N}_{28}} \right)^{.415} \times 10^{-24}$	=	0.726
$\eta f = \nu \frac{\Sigma_f}{\Sigma_{a(total)}}$	=	1.9692
$k_\infty = \eta f p \epsilon$		1.4296
$= \frac{\sum_i \Sigma_{s_i} \bar{\xi}_i}{\Sigma_s}$	=	0.17598
$\tau = \frac{D}{\Sigma_s} \ln \left(\frac{E_1}{E_2} \right)$	=	343 cm^2
$B^2 = \left(\frac{2.405}{R + d} \right)^2 + \left(\frac{\pi}{H+2\delta z} \right)$	=	1.332×10^{-3} cm^2
β = albedo of Beryllium		
$k_{eff} = \frac{k_\infty e^{-B^2 \tau}}{1+B^2 L^2}$	=	0.894

Application of the Flux Equations

The S_n approximation is a method of differencing in which the independent variable is quantized into n intervals, and intermediate values of a function of the variable are approximated by a straight line between points at the boundaries of the interval. This method of numerical integration was developed by Bengt G. Carlson[6].

The vector flux at a point within a reactor can be obtained by the use of the S_2 method. The equations necessary are derived in Appendix A for two cases of neutron velocity:

Case A - The component of the vector flux in the axial direction is greater than its component in the radial direction.

Case B - The component of the vector flux in the radial direction is greater than that in the axial direction.

These two cases are illustrated in Figure I using a grid which is used to difference the transport equation in the r and z coordinates, r being the radial coordinate and z the axial coordinate.

Figure I

The two cases of flux at a grid point

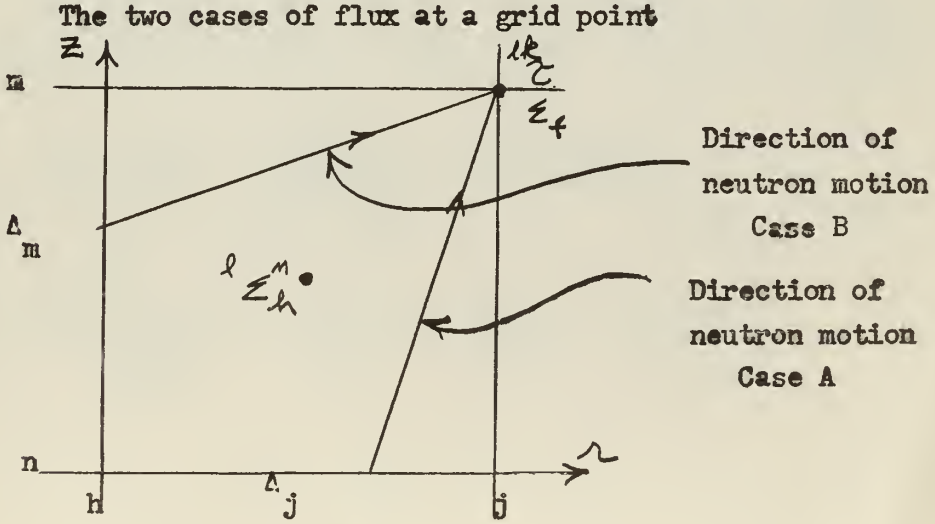

The general flux equation for case A is:

$$\ell\phi^{i,f}_{j,m} = \frac{|b_i|\,(1-\omega^{i,f})\left(\ell\phi^{i,f}_{j,n} + \ell\phi^{i-1,f}_{j,n} - \phi^{i-1,f}_{j,m} + \omega^{i,f}A_2\right)}{|b_i| + \omega^{i,f}\frac{|\Delta_j|}{2}\left(g_f\,\ell\Sigma^n_h + \frac{c_i}{r_h}\right)} \qquad (1)$$

where h is a value which is one greater or less than j, depending upon the direction of the radial component of vector flux, and n is a value which is one greater or one less than m, depending upon the direction of the axial component of vector flux. Definitions of the other quantities can be found in the nomenclature part of this section.

For case B the flux at a point is defined by the following equation:

$$\ell\phi^{i,f}_{j,m} = \frac{|b_i|(1-\omega^{i,f})\left(\ell\phi^{i,f}_{h,m} + \ell\phi^{i-1,f}_{h,m} - \ell\phi^{i,f}_{h,m} - \ell\phi^{i-1,f}_{h,n}\right)}{|b_i| + \frac{|\Delta_j|}{2}\left(g_f\,\ell\Sigma^n_h + \frac{c_i}{r_h}\right)} \qquad (2)$$

where A for Equation (1) and (2) is defined by:

$$A = \left[|b_i| - \frac{|\Delta_j|}{2}\left(g_f\,\ell\Sigma^n_h + \frac{c_i}{r_h}\right)\right]\ell\phi^{i,f}_{h,n} - \left[|b_i| + \frac{|\Delta_j|}{2}\left(g_f\,\ell\Sigma^n_h - \frac{c_i}{r_h}\right)\right]\ell\phi^{i-1,f}_{j,m}$$
$$+ \left[|b_i| - \frac{|\Delta_j|}{2}\left(g_f\,\ell\Sigma^n_h - \frac{c_i}{r_h}\right)\right]\ell\phi^{i-1,f}_{h,h} + \frac{e_i\,g_f|\Delta_j|}{2}\left[\ell S_{j,m} + \ell S_{h,n}\right]$$
$$+ \left[\frac{|b_i| - |d_i|}{2}\right]\left[\ell\phi^{i-1,f}_{j,m} + \ell\phi^{i-1,f}_{j,n} - \ell\phi^{i-1,f}_{h,m} - \ell\phi^{i-1,f}_{h,n}\right] \qquad (3)$$

It should be pointed out that the total macroscopic cross section, Σ, is evaluated using the material properties at the center of the position grid of Figure I, but are designated by the grid values at the corner diagonally opposite the point j,m, i.e.; the point h,n. Further, $\bar{r}_h$ is actually the mean radius and is equal to $\frac{r_j + r_h}{2}$.

The source at a point is defined by the following equations

$$\ell S_{j,m} = \nu \ell p \sum_{k=1}^{3} k\Sigma_f \, k\phi_{j,m} + \sum_{k=1}^{3} \ell k \tau \, k\phi_{j,m}$$

where the scalar flux $\phi_{j,m}$ is equal to

$$\sum_{f=0}^{1} H_f \sum_{i=o}^{2} P_i \, \ell \phi^{i,f}_{j,m}$$

The fission cross section and transfer probabilities, τ, are evaluated using the material properties at the grid point at which the flux is being calculated. The data necessary for the solution of the flux at a point is summarized in Tables I and II.

Table I.

Data for the S_2 approximation

i	ℓ_i	b_i	c_i	d_i	e_i	P_i
0	-1	-1	0	--	1	+0.3183
1	0	-1/3	4/3	-2/3	2	+0.3643
2	1	2/3	4/3	1/3	2	+0.3183

Table II.

Data for Gauss quadrative approximation

f	μ_f	h_f	g_f	H_f
0	-0.8611363	-1.6944625	+1.9677054	+0.3478548
1	-0.3399801	-0.3197284	+1.063340	+0.6521452
2	+0.3399801	+0.3197284	+1.063340	+0.6521452
3	+0.8611363	+1.6944625	+1.9677054	+0.3478548

Not all pairs of values for i and f are relevant for each of the cases A and B as a consequence of the defining inequalities for these cases. The pairs of relevant values are discussed in connection with Figure II. A general point may be defined to be any grid point of the reactor other than a point at the center, on the centerline or in the midplane of the reactor. A point at these other places is called an origin point, a center-line point or a midplane point, respectively. For Case A for which $|b_i| < |h_f|$ and in the case of the first quadrant flux, there is a further requirement (Table I, Appendix A) that b_i and H_f have negative signs. In this quadrant there are three Case A flux equations, one for each of the pairs (i=0, f=0), (i=1,f=0), and (i=1,f=1). Similarly, for Case B, the requirement $|b_i| > |h_f|$ leads to only one relevant combination.

The applicable combinations and those for the remaining three quadrants are summarized in Table III.

Figure II

Flux Configuration
for a particular energy group
at a general grid point

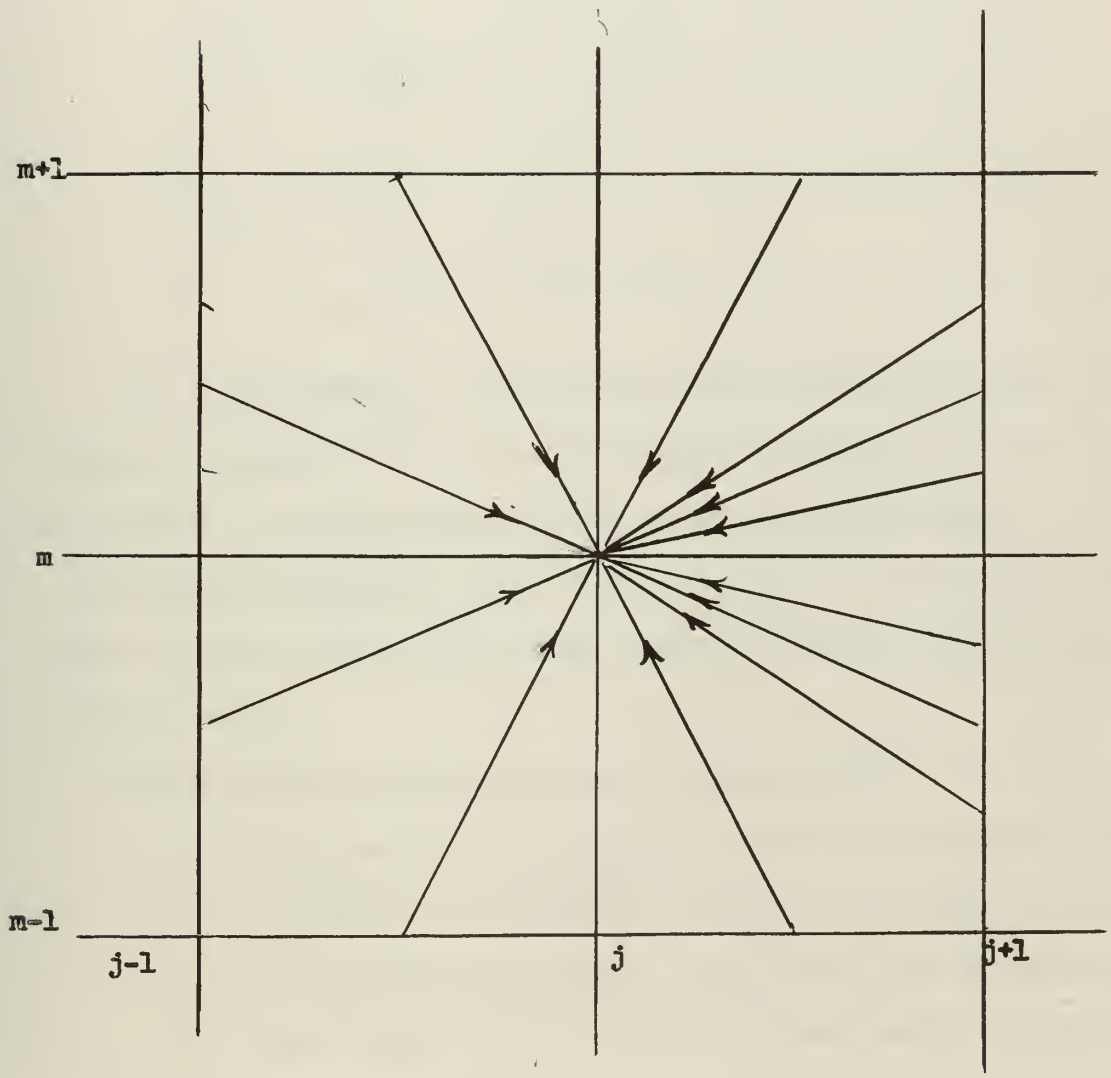

Table III

Allowable combinations of i and f

Quadrant	Case A	Case B
1st	i = 0, f = 0 i = 1, f = 0 i = 1, f = 1	i = 0, f = 1
2nd	i = 2, f = 0	i = 2, f = 1
3rd	i = 2, f = 3	i = 2, f = 2
4th	i = 0, f = 3 i = 1, f = 3 i = 1, f = 2	i = 0, f = 2

The configuration of the flux at a grid point which results from the allowable combinations of i and f are shown in Figure II. If the flux is assumed to be distributed in $\ell+1$ energy groups there will be 12 $(\ell+1)$ flux equation associated with every grid point. For the case considered, there are three energy groups and, therefore, thirty-six flux equations for each point.

The following boundary conditions are assumed:[7]

1. Continuity of flux exists at the centerline and at the midplane of the reactor, and further the flux is symmetrical about these boundaries. This permits the calculation of the flux in only one quarter of the reactor. Figure III shows the flux distribution at these various special points.

Figure III

S_2 approximation to the vector flux distribution at the boundary points in a reactor

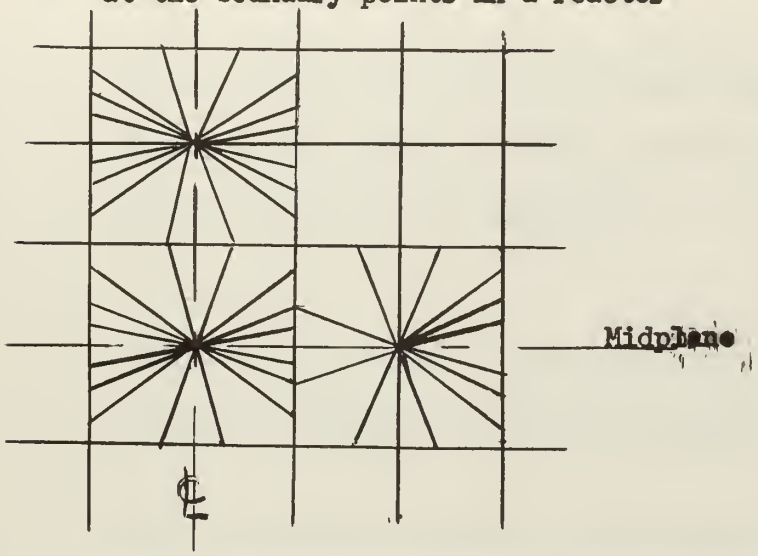

2. A second boundary condition is that at the outside boundaries of the reactor there exists no inward flux. In order to satisfy this requirements, an extra set of grid points is placed just outside these boundaries, and at these points the vector flux whose argument describes inwardly moving neutrons is assumed to be zero. Note, however, that leakage does exist at these fictitious points and at the outside boundary points of the reactor.

Nomenclature

b_i, c_i, d_i, e_i — Values obtained by differencing and integration of the transport equation over η, and defined by Equation (7a to 7d) of Appendix A

g_f, h_f — Values depending upon the quantized values of μ and defined by Equation (7e and 7f) of Appendix A.

H_f — Values obtained by the use of the Gauss quadrature approximation to sum the flux over μ space. defined by Equation (13) Appendix A.

P_i — Values obtained by the use of the S_2 approximation to sum the flux over η space, defined by Equation (12) Appendix A.

$\bar{r}_h$ — mean radius between two adjacent grid points

S — Neutron source

l_p — Fraction of fission neutrons which are produced in a particular energy group l.

ν — Number of neutrons produced per fission.

ℓk_τ	The probability per unit length of neutron travel that a neutron is scattered in group k and that a neutron emerges in group ℓ from the scattering event.
Σ_f	Macroscopic fission cross section
Σ	Total Macroscopic cross section
$\phi(r,z,\mu,\eta,v)$	neutron flux which is classified according to speed, v, colatitude and azimuthal direction, cosines μ and η, and position r and z.
Δ_j	spacing of grid in the radial direction.
Δ_m	spacing of grid in the axial direction.
μ	cosine of the angle Θ between the axis and the direction in which neutrons move. See Figure I Appendix A.
η	Cosine of the angle ψ. See Figure I Appendix A.
ω	See defining equation, page A-12 Appendix A.
ω'	See defining equation, page A-17 Appendix A.

Nomenclature

Superscripts and subscripts

i	index labeling the quantized values of η .
f	index labeling the quantized values of μ.
j	grid position index in the radial direction.
m	grid position index in the axial direction.
ℓ	neutron speed index.
k	neutron speed index of group in which neutron is scattered.
n	axial grid position diagonally opposite grid point at which flux is being calculated.
h	radial grid position.

A computer program is a sequence of logical instructions telling the computer what mathematical operations are to be performed on the data. Therefore, there are two groups of inputs, the data and the instructions. The data fed into the computer are stored in the fast, core memory if there is sufficient room. When the space is not adequate, some of the data are stored in magnetic drums. The only difference in the two storage processes is that the data in the drum takes longer to locate and bring into the core memory. Each number or piece of data is stored in a register or cell the location of which is designated by a number called the address of that register. The instructions are stored in sequence and are performed in the order in which they are stored unless the program directs otherwise. No unused registers are permitted to interrupt the storage as these will stop the computer.

The instructions given to the computer consist of two parts, the operation and the address sections. The operation section is first and uses letters to tell the computer the mathematical operation to be performed. The address section gives the address of the register containing the data on which the operation is to be performed. The instructions recognized by Whirlwind I are listed in the glossary.

For Whirlwind I there are many useful devices that make the programming much simpler. A few of these devices used in this program are floating addresses, preset parameters, and subroutines.

Probably the most useful device is the floating address. This floating address or "flad" is used to eliminate the necessity of referring to the absolute register address in the core memory when

writing the program. The absolute register address of any part of the program must be known primarily so that the initial or final instruction of data is not placed in a register containing part of the subroutines fixed in the memory of the computer.

In the program key instructions on which mathematical operations are to be performed or which will be referred to later in the program are given floating addresses. These addresses consist of a letter and a number, for example a1, a2, etc. Any letter except o and ell may be used and the sum of all the numbers following these letters may not exceed 255. When the program is read into the computer, it will assign absolute addresses or register numbers to these flads. A table of the floating addresses is produced by the computer with the solution unless it is specifically suppressed in the computer. This table gives the absolute address of every assigned floating address and is particularly helpful in trouble shooting a faulty program.

Another useful device is the preset parameter. These are numbers other than data that are used in the program. Preset parameters are frequently used to designate the number of times that a calculation is to be performed. Preset parameters must be assigned a value before they are used, and they will retain this value until it is specifically changed. Preset parameters are designated by two letters and a number. The first letter must be a p, u or z and the second letter and the number may be anything, except the letters o and el may not be used.

A third useful device is the subroutine. Its usefulness comes from the fact that it is a complete entity in itself and may be constructed and trouble shot independently. For the build up of a complete

program it is possible to start with one of the most basic mathematical operational sequences that will be performed repeatedly, program it, perform the hand calculations of the sequence and then place the routine on the computer. Modification of the subroutine or correction of the hand calculations must continue until the results of both are in agreement.

In arranging these subroutines in the main program extreme care must be used. The main program must be interrupted to call the subroutine into use and after the subroutine has performed its function it must direct the computer back to the proper place in the main program.

An example of a subroutine is as follows:

Main program

```
  .
    .
      .
    isu p 10
tl,  isp x 4          take the next instruction from register
                      x 4 and continue from there
     imr a 5          forms product of (-m2) and (a5)
  .
    .
      .
     i STOP           end of program
x4,  ita x 5          transfer into the address section of the
                      instruction in register x5, the address
                      that is one more than the address tl.
     ica m 2)
             )        places m 2 in a 7
     its a 7)
```

	ics m 2 its a 8	places -m 2 in a 8
x5,	isp 0	returns to main program one register after t 13 i.e., register containing imr a 5.

Since the numbers used in this program were over four decimal digits in length, floating point arithmetic was required. In this system two registers are required to express a number. Each of these registers is capable of containing 16 bits of binary number information. The first bit of the first register expresses the sign of the number and the first bit of the second register expresses the sign of the exponent of 2. Six bits are required to locate the binary point of the number leaving 24 bits to express the actual number. In certain stages of the program it is desirable to handle single length register numbers. The instructions for the handling of these numbers are similar to those for double length registers except that the i does not precede the instruction. When operating on double length registers the computer is said to be in the interpretive mode, when on single length registers it is in the Whirlwind mode. To enter the interpretive mode from the Whirlwind mode it is necessary to use the instruction "IN" and to reverse the direction it is necessary to use the instruction "OUT".

GLOSSARY OF INSTRUCTIONS

TERM	DEFINITION
ica x	clear MRA and add contents of register x.
ics x	clear MRA and subtract contents of register x.
iad x	add contents of register x to what is in MRA.
isu x	subtract contents of register x from what is in MRA.
imr x	multiply what is in MRA by the contents of register x and round off product to fifteen digits.
idv x	divide contents of MRA by the contents of register x.
its x	transfer the contents of the MRA to register x losing what was previously in register x. The MRA remains unchanged.
iex x	exchange the contents of the MRA with the contents of register x.
isp x	take the next instruction from register x. Does not affect the contents of the MRA. An unconditional instruction used to break the sequence of operations.

Glossary of Instructions (Continued)

TERM	DEFINITION
icp x	if the contents of the MRA are negative, take the next instruction from register x and continue from there. If the contents of the MRA are positive, take the next instruction in sequence. A conditional instruction used to break the sequence of operations.
isc x	select counter number x. Without this instruction counter zero will be used whenever +C appears.
icr x	cycle reset. Sets index register of counter to zero and criterion register to x.
ict x	cycle transfer. Increases contents of index register by one. If contents of index register greater or equal to contents of criterion register, set index register to zero and do next instruction in sequence. If contents of index register less than contents of criterion register, take next instruction from register x.
ici x	increase the contents of index register by number x.
icd x	decrease the contents of index register by number x.

Glossary of Instructions (Continued)

TERM	DEFINITION
iti x	transfer the right eleven digits of the index register into the right eleven digits of register x.
iat x	add contents of index register to the contents of register x and store the result in the index register and register x.
ita x	replace the address section of the instruction in register x with the address that is one more than the address of the register containing the last isp or icp if the contents of the MRA are negative.
iTOA	record the contents of MRA on direct printer (typewriter).
iMOA	record the contents of MRA on magnetic tape for delayed printing.
iSOA	record the contents of MRA on oscilloscope for photographing.
iFOR	this instruction provides an automatic device for obtaining a suitable layout of output data in columns, lines or blocks.

Note: The above output instructions are usually followed by a series of letters and numbers that indicate the desired form and arrangement of the output.

Computer Logic

The program starts at 1 in the main program by entering the data, program and preset parameters. The initial calculations are with the reactor radius equal to the value placed in register r4. With this radius the program then shifts to the flux iteration and convergence test, 4. In this routine parameters are set to control the number of iterations allowed at one radius and to traverse the computer thru all points in the reactor. With a value of j and m, defining a point in the reactor, the program shifts to Flux, 4.5, where the addresses on the drum of the required data are calculated, the data entered in the fast memory and the routine appropriate to the point is selected and control is shifted to that routine.

The first calculation at any point is the scalar flux for all three groups and the second is the input from fission and scattering from an upper energy group. The first point to be calculated in each cycle is the origin. This is the point of normalization of the inputs to the fast group. The normalization constant, γ, is defined as the reciprocal of the fast group input at the origin. With this constant all other inputs (all groups and all points) are normalized.

As explained in the previous section of the procedure certain quadrants of the flux are required for each point depending on its location. Prior to sequencing to another point all fluxes appropriate are calculated.

The fast source input is then compared to the previous fast source input. If the new value is not within a set specified fractional value of the previous value a negative quantity is introduced into s 10.

When the entire grid has traversed a check is made to see if the maximum allowable attempts at source convergence have been made. If this maximum number has been made the computer will stop. If not a check will be made of switch s 10. As indicated in routine 4, another cycle will be made thru the reactor if s 10 is negative, and if s 10 is positive control will return to the main program to repeat the above procedure based on the radius placed in r 3.

When a gamma is calculated for this radius, control is again returned to the main program but at a different point. All subsequent returns are at this point. A check is made to determine if the maximum allowable number of iterations of radii have been attempted.

A test for criticality is made to see if gamma is within a specified tolerance of unity. If it is not, a new radius is found by extrapolation or interpolation based on the most recent values of R and γ and the best previous value of R and γ. In this determination of radius, the gamma that is closer to unity and the associated radius are preserved for use in later extrapolation. The previously outlined calculations are repeated with this radius. If γ lies within the specified tolerance of unity control remains in the main routine and the print-out routine, which has been stored in the drum, is entered into the fast memory.

The computer is then sequenced thru the grid calculating and printing out scalar fluxes at each point for each group.

If the flux pattern is not as desired the properties of the regions are changed and a new tape of data cut. The program is then run again to determine the flux pattern.

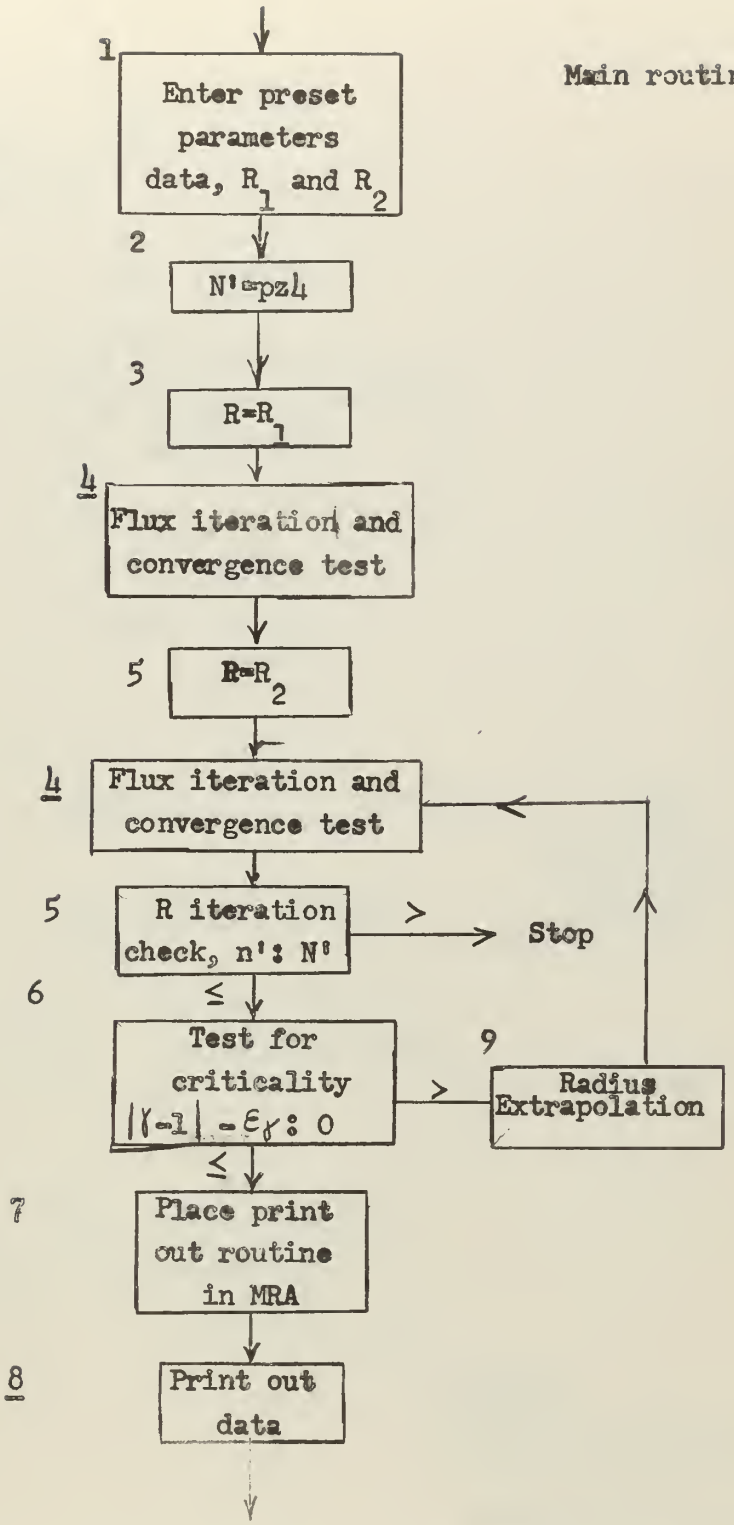
Main routine
1
Enter preset parameters data, R_1 and R_2
2
N'=pzl4
3
R=R_1
4
Flux iteration and convergence test
5
R=R_2
4
Flux iteration and convergence test
5
R iteration check, n': N'
>
Stop
6
≤
Test for criticality
|γ-1| - ε_γ: 0
9
>
Radius Extrapolation
≤
7
Place print out routine in MRA
8
Print out data

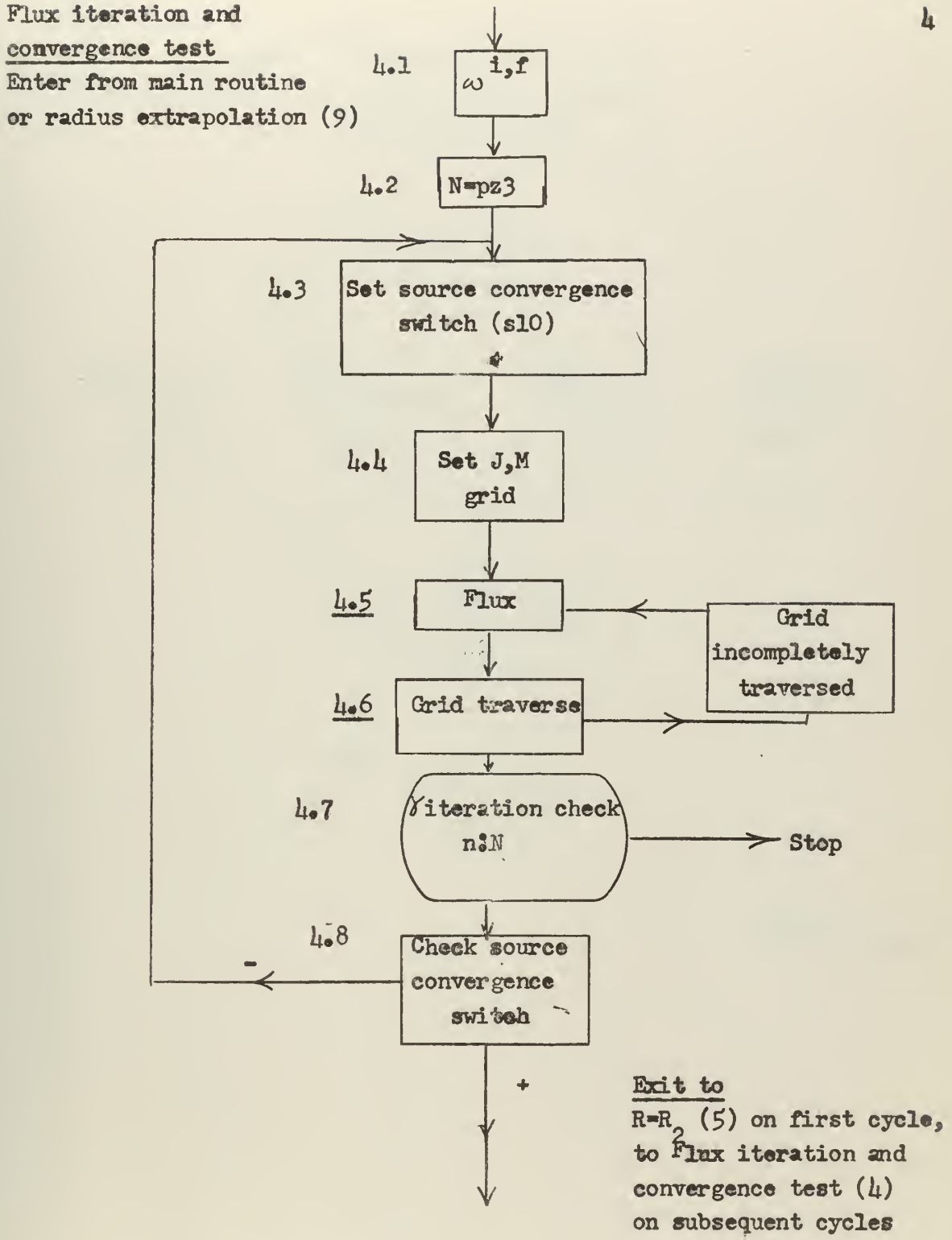
Flux iteration and convergence test
Enter from main routine or radius extrapolation (9)
4.1
$\omega^{i,f}$
4.2
N=pz3
4.3
Set source convergence switch (s10)
4.4
Set J,M grid
4.5
Flux
Grid incompletely traversed
4.6
Grid traverse
4.7
γ iteration check n≥N
Stop
4.8
Check source convergence switch
-
+
Exit to
R=R2 (5) on first cycle,
to Flux iteration and convergence test (4)
on subsequent cycles

Flux

Enter from Set J,M grid (4.4) or Grid Traverse (4.6)

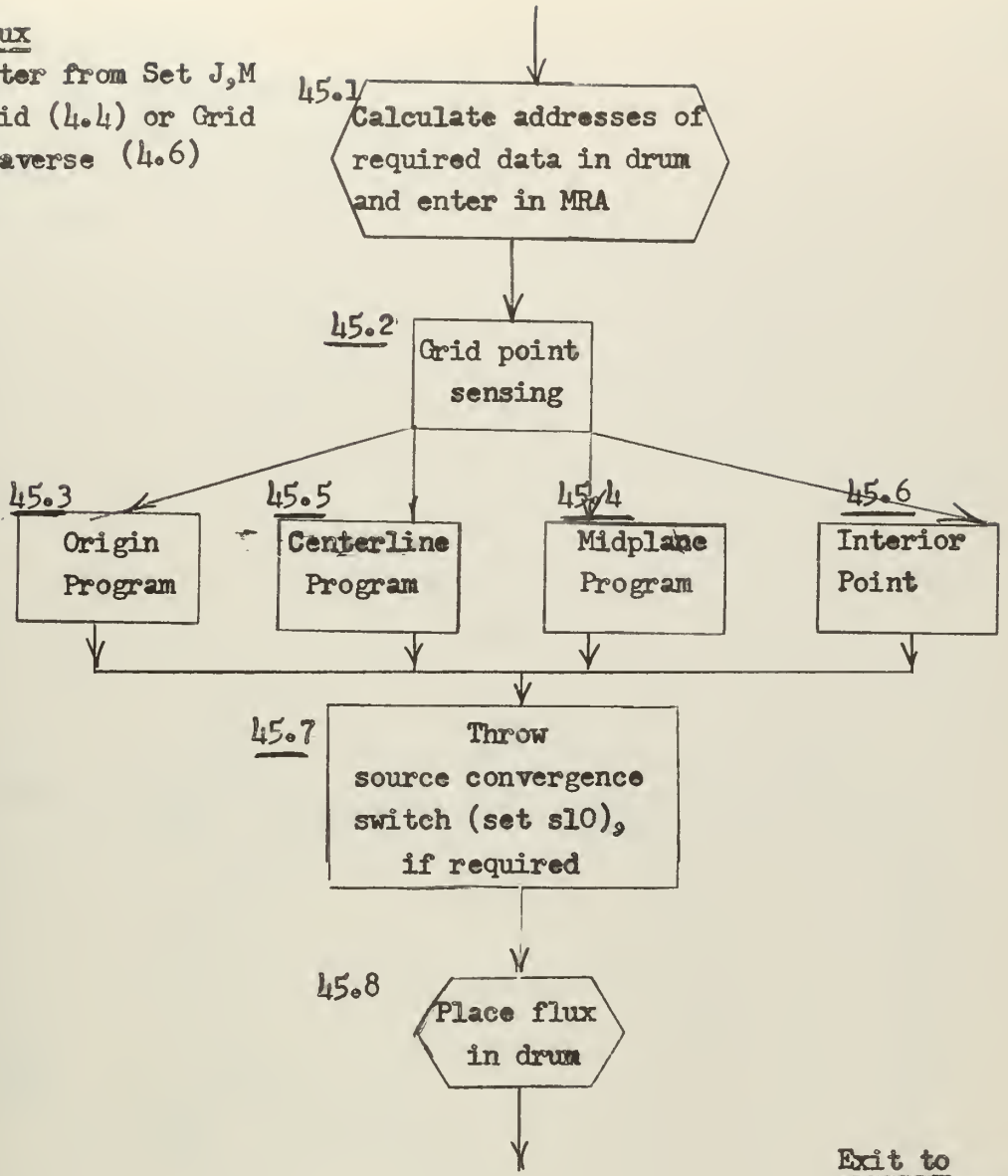

Exit to

Grid traverse (4.6)

Grid Point Sensing

Enter from Address calculation and data entry (45.1) or calculate drum address of required data and enter data (8.1)

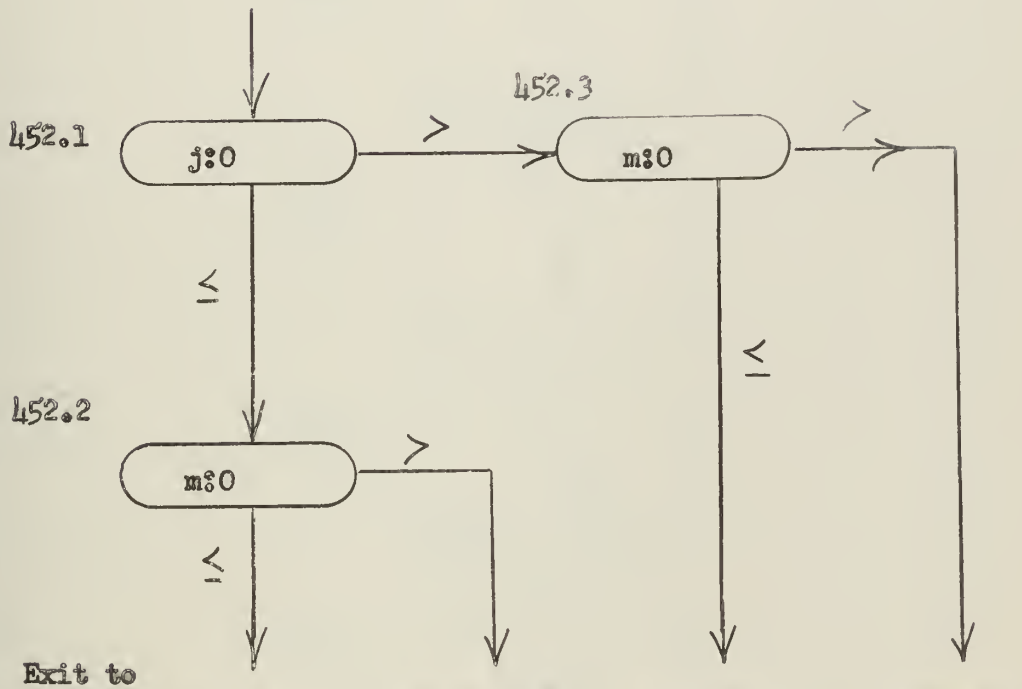

Origin program

Enter from Grid Point Sensing (45.2), origin exit

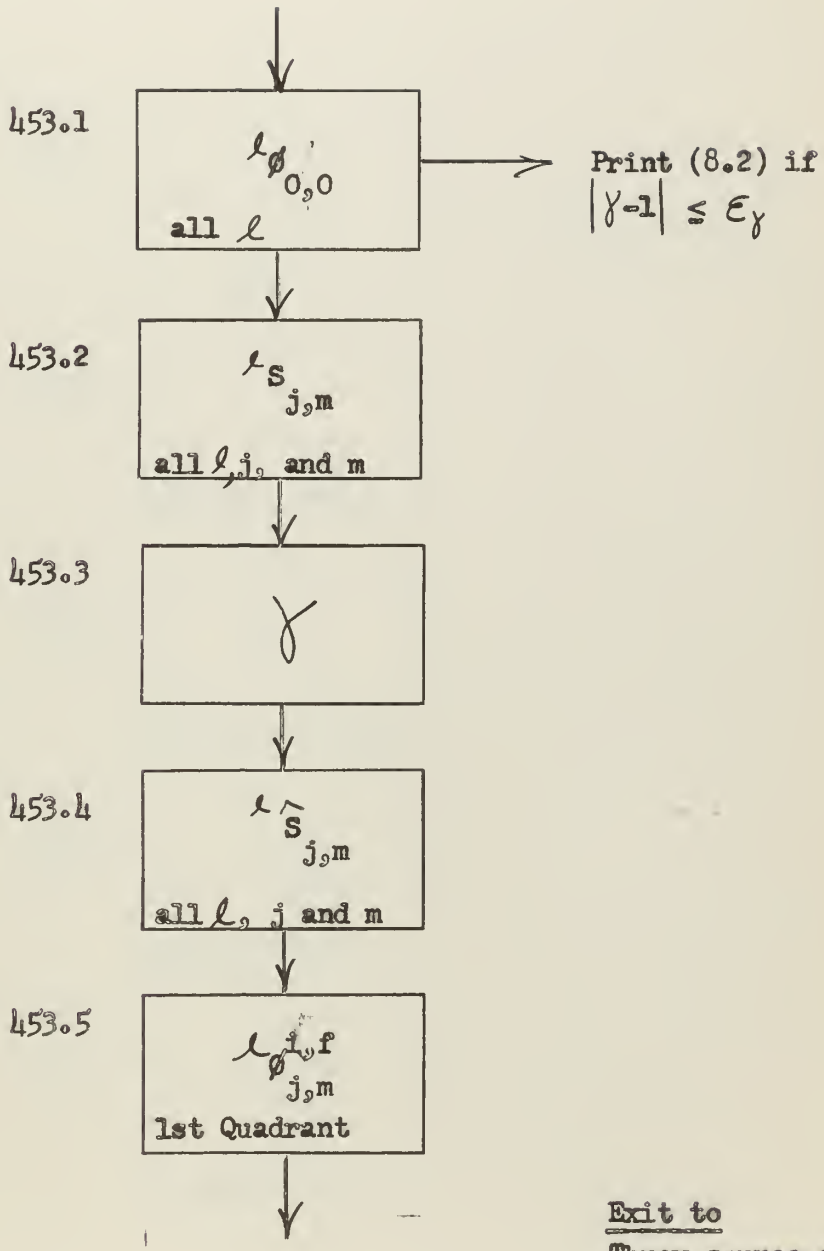

Exit to

Throw source convergence switch (45.7)

Midplane program

Enter from Grid Point Sensing (45.2), midplane exit

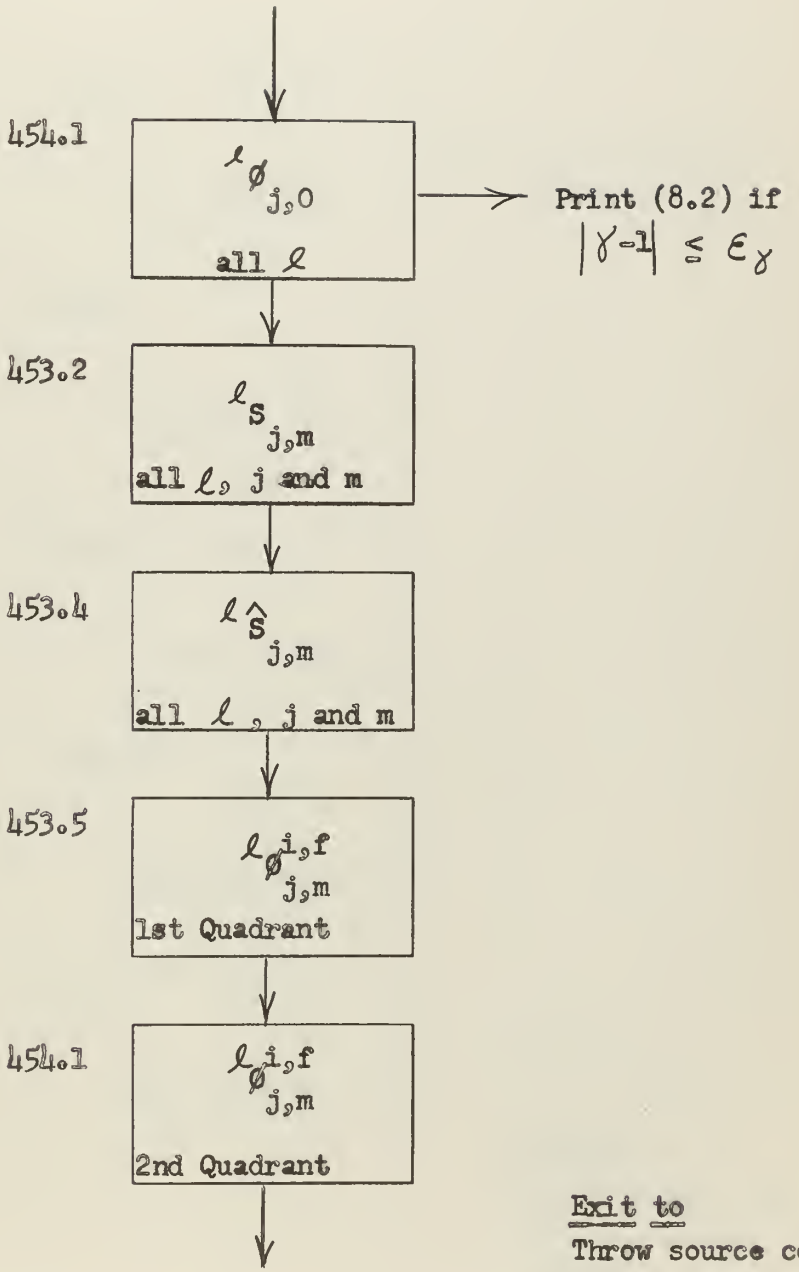

Exit to

Throw source convergence switch (45.7)

Centerline program

Enter from Grid Point

Sensing (45.2), centerline

exit

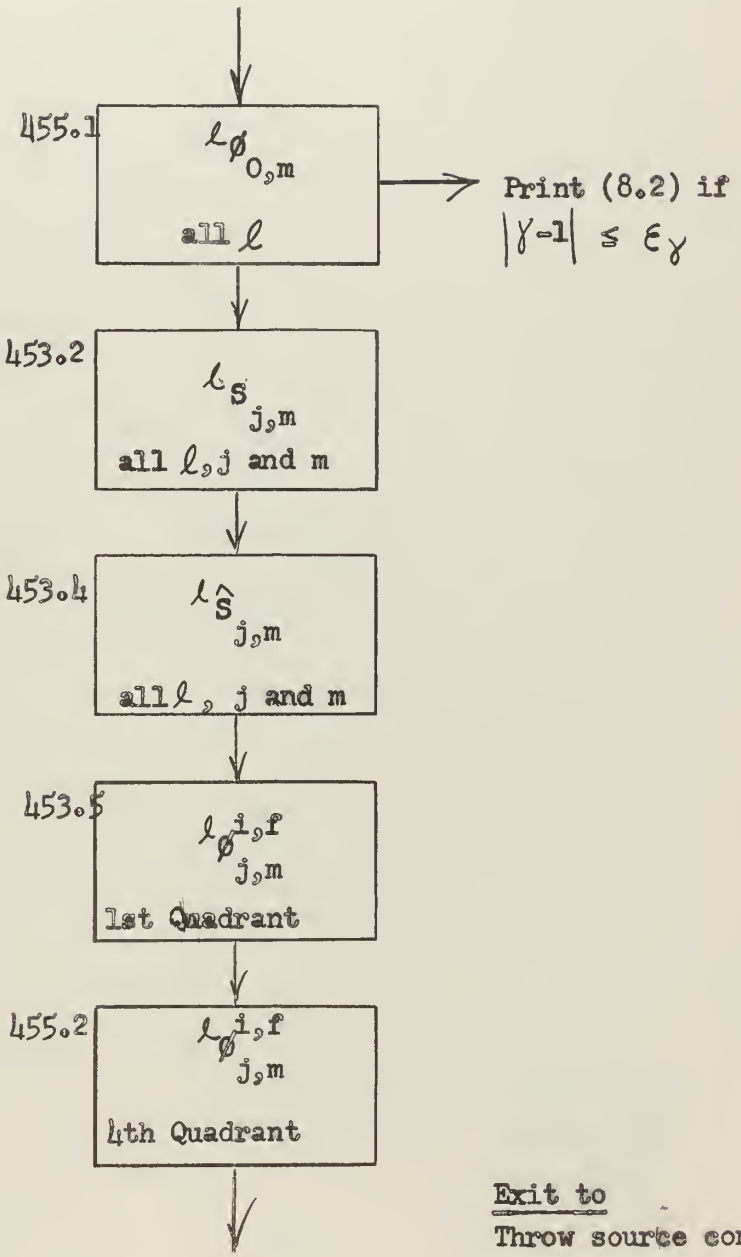

Interior point program

Enter from Grid Point sensing (45.2), general point exit

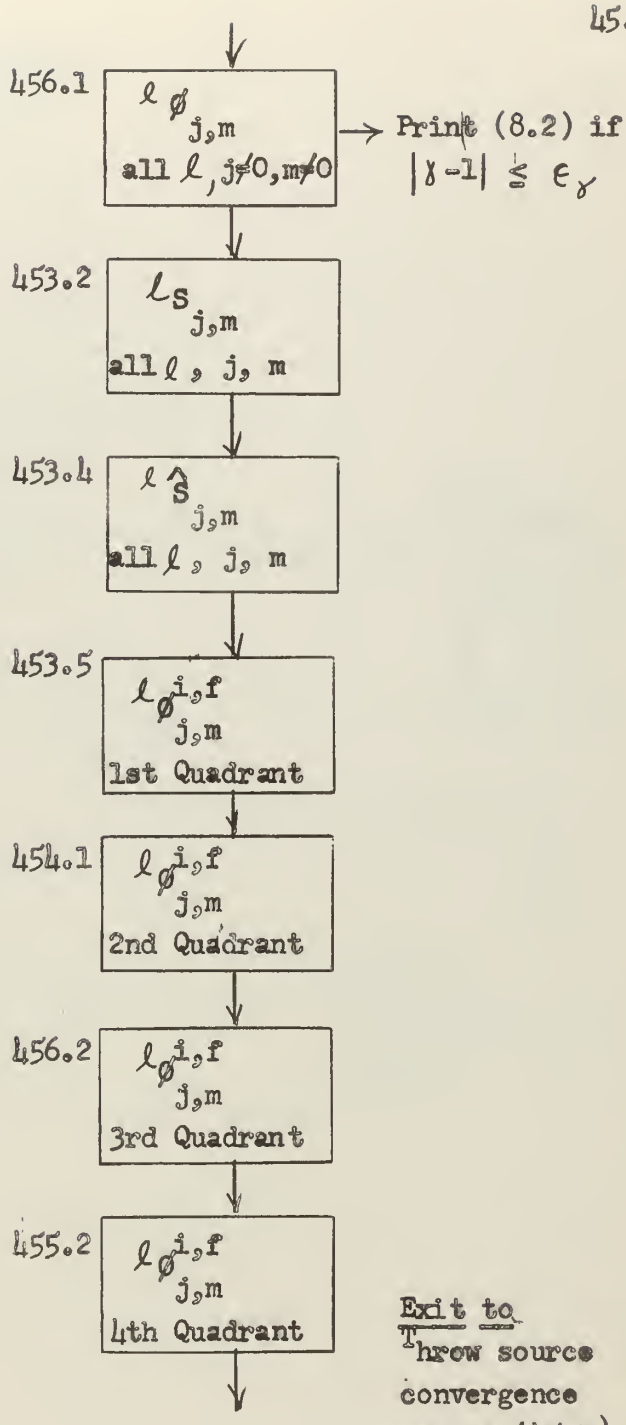

Throw source convergence switch

Enter from origin, midplane, centerline or interior point programs (45.3 to 45.6)

45.7

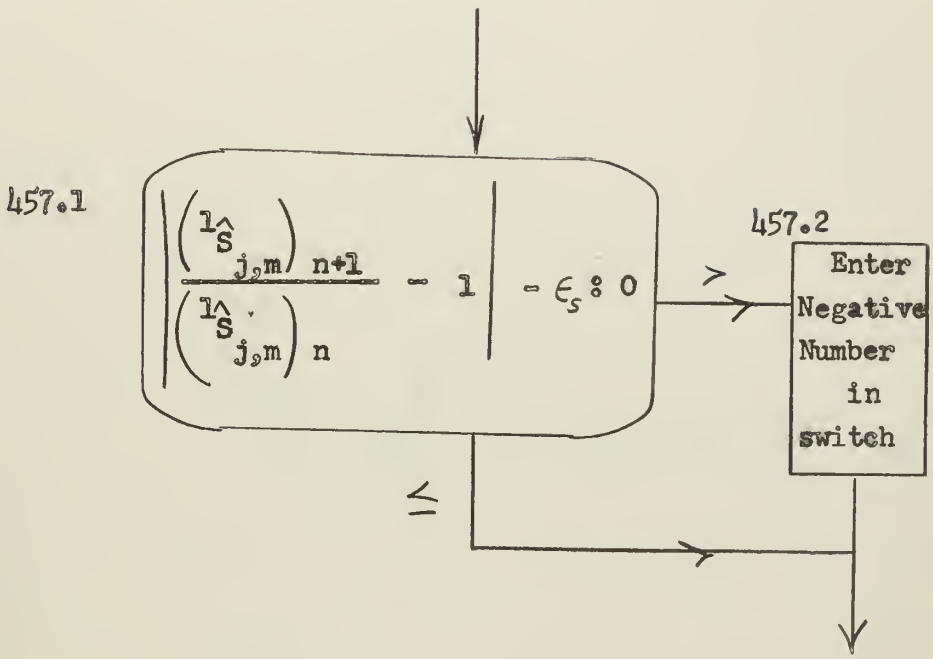

Exit to

Place flux in drum (45.8)

Grid Traverse

Enter from Flux (4.5)
or Print (8.2)

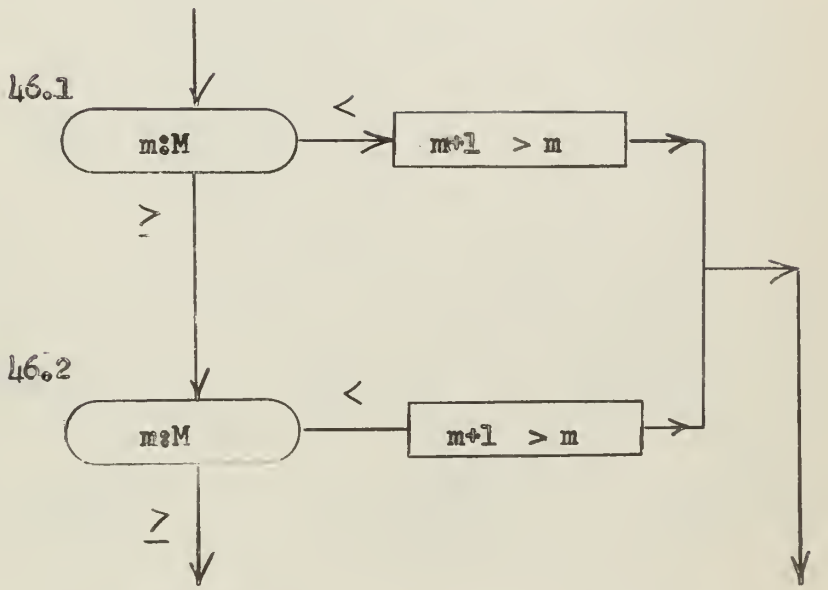

Exit to
γ iteration check (4.7)
or Stop

Exit to
Flux (4.5) or
Drum address
calculation
(8.1)

Print out routine

Enter from place print out routine in MRA (7)

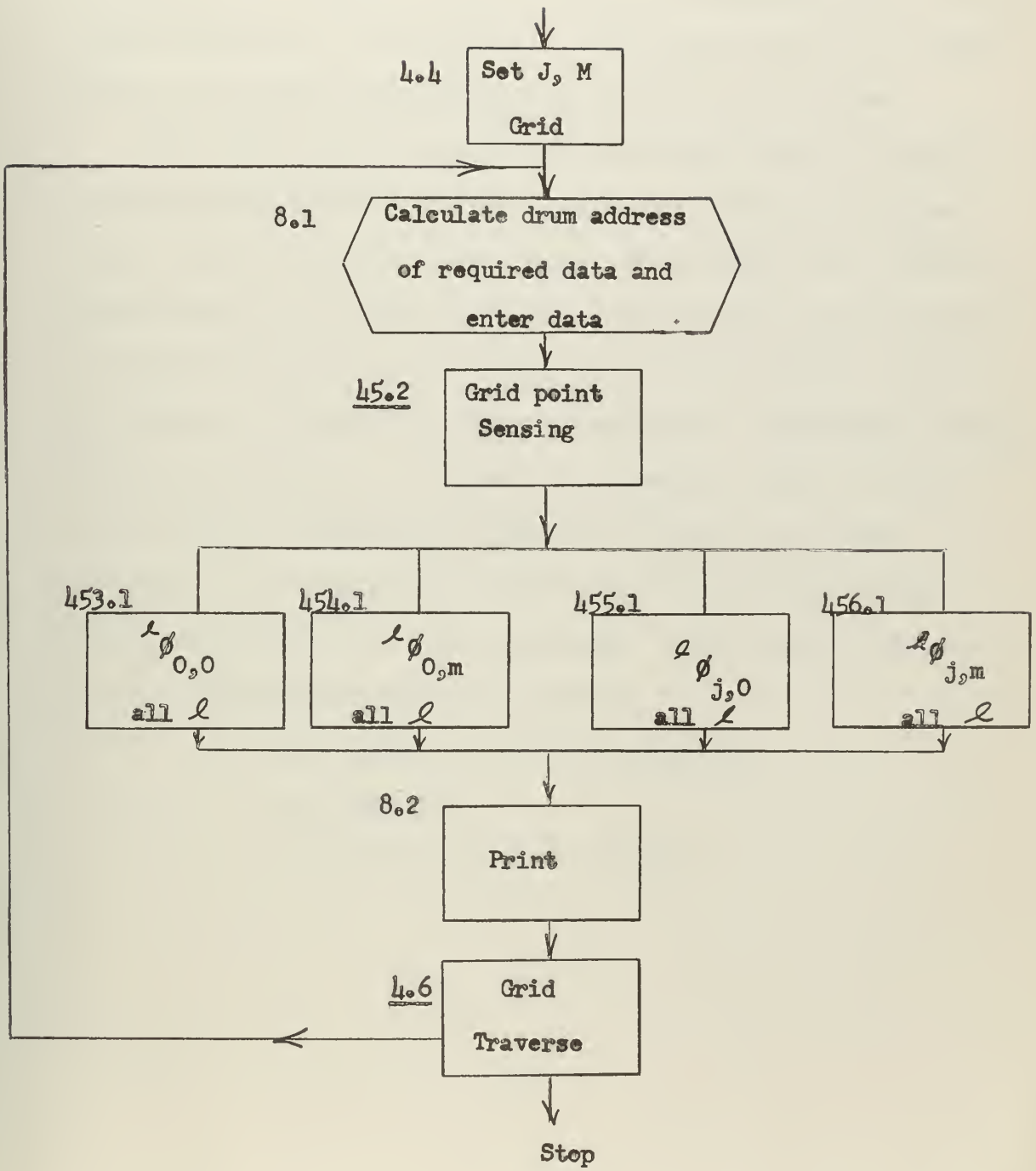

RESULTS

Numerous runs of subroutines and of the entire program were made on Whirlwind with the program contained in Appendix B. This program was adapted for a reactor radius of 75 and 95 centimeters and a height of 168 centimeters. The grid placed on the reactor was a 6 by 6 grid giving for the first trial radius a grid size 15 cm by 34 cm.

The final run had programmed a first trial radius of 75 cm; the maximum allowable number of iterations with a constant radius was twenty and the tolerance of convergence of the fast source input was three percent. The computer stopped, as programmed, upon completion of twenty iterations at a set radius when the fast neutron input at all points was not with the tolerance specified. The computer running time per iteration is two minutes. The computed values of scalar flux at each point and energy group were printed out for each iteration. The normalizing constant decreased from 0.27 for the first iteration to 0.01 for the twentieth. Some values of the scalar flux at the following point were negative

a) interface of core and reflector,

b) reflector,

c) outside boundary of reflector.

DISCUSSION OF RESULTS

The negative values computed for scalar fluxes are known to be unrealistic. The possible causes of this error are

1) improper programming of the theoretically derived flux equation,

2) grid size being excessive.

The theoretical background for the flux equations is sound, and these equations have been programmed for other geometrical arrangements on other computers and give correct flux distributions [11]. The need for a complete hand calculation is well realized, but due to lack of time these hand calculations were not completed fully. Therefore, there is no reason to assume or expect that these equations have been programmed correctly. To accomplish the required hand calculations, computer verification of the hand calculations, and program trouble shooting it is estimated that another three to four weeks full time would be required.

For accuracy in evaluation of neutron transport equations, the grid spacing should be less than or approximately equal to the mean free path of the neutron. If this condition does not prevail, the accuracy and reliability of the calculations decrease rapidly.

A two fold increase in the number of grid points will increase the time of computation by a factor of eight. Any increase in the time required for one iteration thru the reactor is not allowable since now two minutes are required.

The code developed is in the 'interpretative' or 'floating point' mode for Whirlwind, for the reason that this mode is simple to learn and to trouble shoot. Whirlwind has also available a 'Whirlwind' or 'fixed point' mode in which the speed is increased by a factor of roughly 35. Use of the fixed point mode would make the two dimensional S_2 calculation on the Whirlwind computer practical.

CONCLUSIONS

1) The code as presently programmed is incorrect.

2) The grid spacing as used is much too coarse. This difficulty is not inherent in the coded program.

3) The mode of computer operation is unsuitable for an iterative process such as this because it results in a code that progresses too slowly.

RECOMMENDATIONS

1) Prior to the use of any computer a formal or semi-formal course in programming should be completed.
2) A grid spacing comparable to the mean free path of the neutron should be selected.
3) The fastest possible mode of calculation on the computer available should be used.
4) For a coded program of this difficulty a faster machine with a much larger fast memory is very desirable.

Appendix A

Development of Equations Using S_2 Approximation to the Boltzman Equation for Cylindrical Geometry

Equations will be developed for the time independent case using cylindrical geometry.

The vector flux at a point in space is a function of two variables; one describes distance along the vertical axis of the cylinder, and the other describes radial distances. The axial variable will be designated as μ and the radial variable as η. From Figure I it can be seen that:

$\eta = \cos \Psi$

$\mu = \cos \Theta$ and

$\sin\Theta = \sqrt{1 - \mu^2}$

$\sin \Psi = \sqrt{1 - \eta^2}$

and where $\hat{\Omega}$ represents the unit vector in which direction neutrons travel at a point. Therefore,

$$\nabla \phi = \hat{i}_r \frac{\partial \phi}{\partial r} + \hat{i}_\Theta \frac{1}{r} \frac{\partial \phi}{\partial \Psi} + \hat{i}_z \frac{\partial \phi}{\partial z}$$

and $\hat{\Omega} = \hat{i}_r \sin \Theta \cos \Psi -$

$\hat{i}_\Theta \sin \Theta \sin \Psi \frac{\partial \phi}{\partial \Psi} + \hat{i}_z \cos \Theta.$

Figure I

Components of neutron flux at a space point.

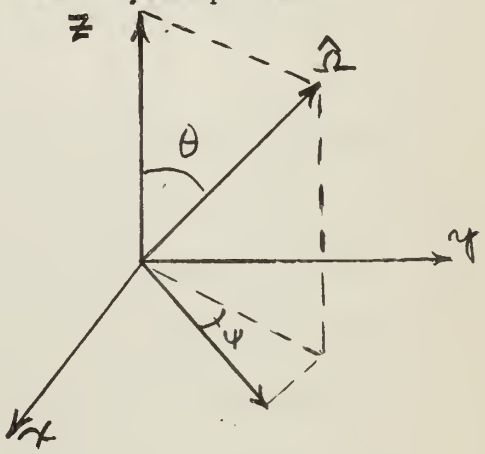

Therefore,

$$\hat{\Omega} \cdot \nabla \phi = \sin \Theta \cos \Psi \frac{\partial \phi}{\partial r} - \frac{\sin \Theta \sin \Psi}{r} \frac{\partial \phi}{\partial \Psi} + \cos \Theta \frac{\partial \phi}{\partial z} . \qquad (1)$$

If we substitute the expression for η and μ which were derived from Figure I in equation 1, we find

$$\hat{\Omega} \cdot \nabla \phi = \eta \sqrt{1-\mu^2} \frac{\partial \phi}{\partial r} + \frac{(1 - \eta^2)}{r} \sqrt{1-\mu^2} \frac{\partial \phi}{\partial \eta} + \mu \frac{\partial \phi}{\partial z} \qquad (2)$$

The quantity $\hat{\Omega} \cdot \phi$ represents the leakage of neutrons out of an element of volume per unit time in the direction $\hat{\Omega}$ per unit solid angle.

In the time independent case this leakage plus the rate of loss of neutrons, $\Sigma\,\phi$, per unit time must equal the source strength, S. In problems in which cross sections vary with energy and neutrons alter their speeds, the multigroup approximation of the Boltzmann equation is introduced: [6]

$$\frac{\partial \ell\phi}{\partial r} + \frac{1-\eta^2}{r}\,\frac{\partial \ell\phi}{\partial \eta} + \frac{\mu}{\sqrt{1-\mu^2}}\,\frac{\partial \ell\phi}{\partial z} = \frac{S}{\sqrt{1-\mu^2}} - \frac{\ell\Sigma\,\ell\phi}{\sqrt{1-\mu^2}}, \qquad (3)$$

where $\ell\Sigma$ is the total cross section within the energy group 'ℓ' and ℓS is the neutron source term which results from fission and energy degradation of the total vector flux at the point. Slowing down is incorporated into the source term.

Equation 3 is identical in form to the time dependent multigroup equation for spherical geometry in which the z term is replaced by a term representing the rate of change of flux with respect to time.

The S_n approximation is a method of evaluating integrals over a variable in which the variable is quantized into n intervals and intermediate values of a function of the variable are approximated by a straight line between points at the boundaries of the intervals. We shall consider η space as the first variable which will be integrated. The flux at any point (r, z, η) in Figure II can be represented by the following equation where i represents the interval number.

Figure II

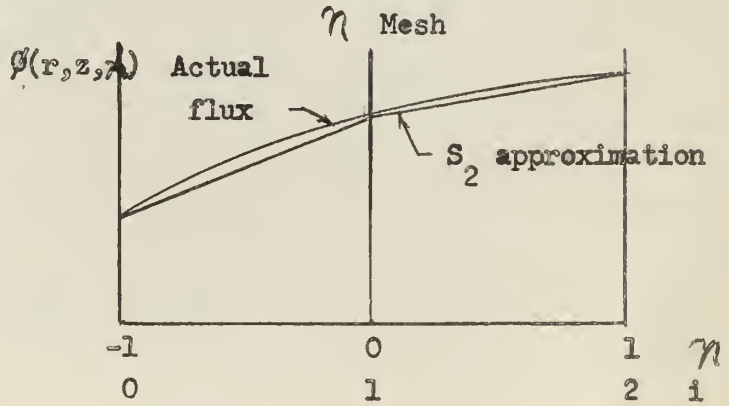

$$\phi(r,z,\eta) = \frac{\eta - \eta_{i-1}}{\eta_i - \eta_{i-1}}\,\phi(r,z,\eta_i) + \frac{\eta_i - \eta}{\eta_i - \eta_{i-1}}\,\phi(r,z,\eta_{i-1}) \tag{4}$$

For the S_2 approximation $i = +1, 0,$ and -1. If we denote $\eta_i - \eta_{i-1}$ as Δ_i and $\phi(r,z,\mu,\eta_i)$ as ϕ^i we obtain

$$\phi = \frac{(\eta - \eta_{i-1})}{\Delta_i}\,\phi^i + \frac{(\eta_i - \eta)}{\Delta_i}\,\phi^{i-1}$$

If we substitute this in equation 3, we find

$$\frac{\eta(\eta - \eta_{i-1})}{\Delta_i}\frac{\partial^\ell \phi^i}{\partial r} + \frac{\eta(\eta_i - \eta)}{\Delta_i}\frac{\partial^\ell \phi^{i-1}}{\partial r} + \frac{(1-\eta^2)}{r}\frac{(\eta - \eta_{i-1})}{\Delta_i}\frac{\partial^\ell \phi^i}{\partial \eta}$$
$$+ \frac{(1-\eta^2)(\eta_i - \eta)}{\Delta_i}\frac{\partial^\ell \phi^{i-1}}{\partial \eta} + \frac{\mu(\eta - \eta_{i-1})}{\sqrt{1-\mu^2}\,\Delta_i}\frac{\partial^\ell \phi^i}{\partial z} + \frac{\mu(\eta_i - \eta)}{\Delta_i}\frac{\partial^\ell \phi^{i-1}}{\partial z}$$
$$= \frac{{}^\ell S}{\sqrt{1-\mu^2}} - \frac{{}^\ell\Sigma(\eta - \eta_{i-1})\,{}^\ell\phi^i}{\Delta_i\sqrt{1-\mu^2}} - \frac{{}^\ell\Sigma(\eta_i - \eta)\,\phi^{i-1}}{\Delta_i\sqrt{1-\mu^2}}\,. \tag{5}$$

Since the source, S, is isotropic, integrating this expression over η from η_{i-1} to η_i, we obtain n equations in the form

$$b_i\frac{\partial^\ell \phi^i}{\partial r} + c_i\frac{{}^\ell\phi^i}{r} + h\frac{\partial^\ell \phi^i}{\partial z} + g\,{}^\ell\Sigma\,{}^\ell\phi^i + d_i\frac{\partial^\ell \phi^{i-1}}{\partial r} - c_i\frac{{}^\ell\phi^{i-1}}{r} +$$
$$+ h\frac{\partial^\ell \phi^{i-1}}{\partial z} + g\,{}^\ell\Sigma\,{}^\ell\phi^{i-1} = e_i\,g\,S\,. \tag{6}$$

where

$$b_i = \frac{2\eta_i + \eta_{i-1}}{3}\,, \tag{7a}$$

$$c_i = \frac{2}{3\Delta_i}\left(3 - \eta_i^2 - \eta_i\eta_{i-1} - \eta_{i-1}^2\right), \tag{7b}$$

$$d_i = \frac{\eta_i + 2\eta_{i-1}}{3}, \qquad (7c)$$

$$e_i = 2 \qquad (7d)$$

$$h = \frac{\mu}{\sqrt{1-\mu^2}}, \qquad (7e)$$

$$g_f = \frac{1}{\sqrt{1-\mu^2}}. \qquad (7f)$$

A different method of finite differencing is used for the other directional variable, μ, since use of an expression analogous to (4) for μ in the integration of the equation (5) with respect to μ would result in an extremely complex expression. Instead, the equation (5) is directly quantized with respect to μ giving the results

$$b_i \frac{\partial \ell\phi^{i,f}}{\partial r} + c_i \frac{\ell\phi^{i,f}}{r} + h_f \frac{\partial \ell\phi^{i,f}}{\partial z} + g_f \ell\Sigma \ell\phi^{i,f}$$

$$d_i \frac{\partial \ell\phi^{i-1,f}}{\partial r} - d_i \frac{\ell\phi^{i-1,f}}{r} + h_f \frac{\partial \ell\phi^{i-1,f}}{\partial z} + g_f \ell\Sigma \ell\phi^{i-1,f} = e_i g_f S \qquad (8)$$

We may now proceed to evaluate the source integral at a point. For isotropic scattering and three energy groups of neutrons

$$S(r,z) = \chi^{\ell}_{p} \sum_{k=1}^{3} {}^{k}\Sigma_f \, {}^{k}\phi(r,z) + \sum_{k=1}^{3} \ell^{k}\tau \, {}^{k}\phi(r,z), \qquad (9)$$

where

$${}^{k}\phi(r,z) = \frac{1}{2\pi} \int_{-1}^{+1} d\mu \int_{-1}^{+1} \phi(r,z,\mu,\eta) \frac{d\eta}{\sqrt{1-\eta^2}}$$

As in equation (4) $\phi(r,z,\mu,\eta)$ is approximated by

$$\phi(r,z,\mu,\ ) = \frac{\eta - \eta_{i-1}}{\Delta_i} \phi^{i}(r,z,\mu) + \frac{\eta_i - \eta}{\Delta_i} \phi^{i-1}(r,z,\mu),$$

and

$$k\phi(r,z,\mu) = \frac{1}{2\pi}\sum_{i=0}^{2}\left\{\phi^{i}\left[\int_{\eta_{i-1}}^{\eta_i}\frac{\eta\,d\eta}{\sqrt{1-\eta^2}} - \eta_{i-1}\int_{\eta_{i-1}}^{\eta_i}\frac{d\eta}{\sqrt{1-\eta^2}}\right]\right.$$

$$\left. + \phi^{i-1}\left[\eta_i\int_{\eta_{i-1}}^{\eta_i}\frac{d\eta}{\sqrt{1-\eta^2}} - \int_{\eta_{i-1}}^{\eta_i}\frac{\eta\,d\eta}{\sqrt{1-\eta^2}}\right]\right\} . \quad (10)$$

Upon integration

$$k\phi(r,z,\mu) = \frac{1}{2}\sum_{i=0}^{2}\left[\frac{\phi^{i}}{\pi\Delta_i}\left\{\sqrt{1-\eta_{i-1}^2} - \sqrt{1-\eta_i^2} + \eta_{i-1}\sin^{-1}\eta_{i-1}\right.\right.$$

$$\left.\left. - \eta_{i-1}\sin^{-1}\eta_i\right\}\right] + \frac{1}{2}\left[\frac{\phi^{i-1}}{\pi\Delta_i}\left\{\eta_i\sin^{-1}\eta_i\right.\right. \quad (11)$$

$$\left.\left. - \eta_i\sin^{-1}\eta_{i-1} + \sqrt{1-\eta_i^2} - \sqrt{1-\eta_{i-1}^2}\right\}\right] .$$

If values of $\eta_i = +1, 0$ and -1 (S_2 approximation) are substituted in the above expression, we find that

$$k\phi(r,z,\mu) = \frac{1}{2\pi}\sum_{i=0}^{2} P_i\,\phi^{i}(r,z,\mu) , \quad (12)$$

where $P_0 = 0.3183$, $P_1 = 0.3634$, and $P_2 = 0.3183$.

By use of the Gauss quadrative method[8] the remaining integral can be evaluated in the form of a sum of the products of coefficient times the vector flux where μ_f values are the n+2 positive roots of

$$P_{n+2}(\mu_f) = 0.$$

The table below lists the values of μ_f and the coefficient H_f used

f	μ_f	H_f
0	-0.8611363	0.3478548
1	-0.3399810	0.6521452
2	+0.3399810	0.6521452
3	+0.8611363	0.3478548

Therefore, since $H_0 = H_3$ and $H_1 = H_2$ the scalar flux at a point is

$$^k\phi(r,z) = \sum_{f=0}^{3} H_f \sum_{i=0}^{2} P_i \, {}^k\phi^{i,f}(r,z), \tag{13}$$

and the source term equals

$$S = \chi^{\ell}_p \sum_{k=1}^{3} {}^k\Sigma_f \, {}^k\phi(r,z) + \sum_{k=1}^{3} {}^{\ell}k_{\gamma} \, {}^k\phi(r,z). \tag{14}$$

where

$^{\ell}_p$ is the propability that a fission neutron will have an energy ℓ and

$^{\ell k}\gamma$ is the probability that a neutron having an energy k will be scattered into the energy group ℓ, $k \geq \ell$.

The scattering probability requires further explanation. We define $\mu_{\ell k}$ as the probability that a neutron which is scattered in the k^{th} group will land in the ℓ^{th} group, k as the energy group in which the scattering occurs (1 for fast, 2 for epithermal and 3 for thermal) and ℓ as the energy group into which the neutron is scattered. The energy range covered by scattered neutrons is $E-\alpha E$, and the probability of landing in the interval ΔE is $\frac{\Delta E}{E-\alpha E}$. Let E be the energy of the neutron before scattering.

$$E_{k+1} < E < E_k.$$

The neutron flux per unit energy interval is $\frac{d\phi}{dE}$.

Then $\frac{d\phi}{dE}\, dE\, \Sigma_s(E)$ is the number of neutrons scattered per unit volume and per unit time, [9] but

$$\frac{d\phi}{dE} = \frac{q}{\Sigma_s E \xi}$$

Therefore, $\frac{d\phi}{dE}\, dE\ \Sigma_s(E) = \frac{q}{\xi}\ \frac{dE}{E}$ (15)

$\frac{E_\ell - E_{\ell+1}}{E(1-\alpha)}$ is the probability a neutron will land in the ℓ th group.

${}^{\ell k}\gamma$ is the number of neutrons scattered in the k th group that land in the ℓ th group. Since the absorption, sources and leakage in a large thermal reactor are small, the slowing down density q, is rather constant over an energy group. This fact is used to compute the number of neutrons scattered from the group k to group ℓ. [10]

The equations for each case are listed below.

Case	Equation
1. $E_{\ell+1} > \alpha E_k$	${}^{\ell k}\gamma = \frac{{}^{k}\Sigma_s}{(1-\alpha)\ [\ln(E_k/E_{k+1})} (E_\ell - E_{\ell+1})(\frac{1}{E_{k+1}} - \frac{1}{E_k})$ (16a)
2. $E_\ell > \alpha E_k$ $\alpha E_k > E_{\ell+1} > \alpha E_{k+1}$	${}^{\ell k}\gamma = \frac{{}^{k}\Sigma_s}{(1-\alpha)\ \ln(E_k/E_{k+1})} \left[\frac{E_\ell - E_{\ell+1}}{E_{k+1}} + \alpha - \frac{E_\ell}{E_k} - \right.$ $\left. - \alpha \ln\left(\frac{\alpha E_k}{E_{\ell+1}}\right) \right]$ (16b)

3. $E_\ell > \alpha E_k$

$E_{\ell+1} < \alpha E_{k+1}$

$$ {}^{\ell}\gamma^{k} = \frac{\Sigma_s^k}{(1-\alpha)\ \ln\left(E_k/E_{k+1}\right)}\left\{E_\ell\left[\frac{1}{E_{k+1}} - \frac{\alpha}{E_k}\right] + \alpha \ln\frac{E_k}{E_{k+1}}\right\} \qquad (16c) $$

4. $\alpha E_{k+1} < E_\ell < \alpha E_k$

$E_{\ell+1} < \alpha E_{k+1}$

$$ {}^{\ell}\gamma^{k} = \frac{\Sigma_s^k}{(1-\alpha)\ \ln\left(E_k/E_{k+1}\right)}\left\{E_\ell\left[\frac{1}{E_{k+1}} - \frac{\alpha}{E_\ell} - \alpha \ln\frac{E_1}{\alpha E_{k+1}}\right]\right\} \qquad (16d) $$

5. $E_\ell < \alpha E_{k+1}$

$$ {}^{\ell}\gamma^{k} = 0 \qquad (16e) $$

For the cases where the scattering occurs within the energy group we find

$E_{\ell+1} > \alpha E_\ell$

$$ {}^{\ell}\gamma^{\ell} = \frac{\Sigma_s^k}{1-\alpha}\left[1 + \frac{E_{\ell+1} - E_1}{E_\ell \ln E_\ell/E_{\ell+1}}\right] \qquad (16f) $$

$E_{\ell+1} < \alpha E_\ell$

$$ {}^{\ell}\gamma^{\ell} = \left[1 - \frac{\xi}{\ln E_\ell/E_{\ell+1}}\right]\Sigma_s^k $$

We may now proceed to evaluate equation 4 by integrating over the r and z variables. However, before doing so we must consider the direction in which integration should be carried out. It is always best to integrate in the direction of neutron flow since any errors produced in the process of integration will be diminished as we proceed further in this direction.

If integration is carried out in a direction opposite to that of neutron flow, any errors produced will be magnified.[7]

We must now difference our equations with respect to r and z. We can arrange terms in equation (8) in order to facilitate the integration. Thus equation (8) becomes

$$\left[h_f \frac{\partial}{\partial z} + b_i \frac{\partial}{\partial r} \right] \left[\ell\phi^{i,f} + \ell\phi^{i-1,f} \right] = -\left[g_f \ell_\Sigma + \frac{c_i}{r} \right] \ell\phi^{i,f}$$

$$-\left[g_f \ell_\Sigma - \frac{c_i}{r} \right] \ell\phi^{i-1,f} + \left[b_i - d_i \right] \frac{\partial \ell\phi^{i-1,f}}{\partial r} + e_i g_f \ell_S \qquad (17)$$

We must now further divide the results of the integration into two separate cases:

Case A - The component of velocity in the r direction is less than the component of velocity in the z direction.

Case B - The component of velocity in the r direction is greater than the component of velocity in the z direction.

If we consider Case A, and difference r and z as illustrated in the figure below, we obtain four distinct subcases. These will be classified in accordance with the direction of travel being determined by the signs of b_i and h_f. A positive sign indicates a direction of travel away from the center of the core. The various cases are listed in Table I.

Figure III
Position Mesh

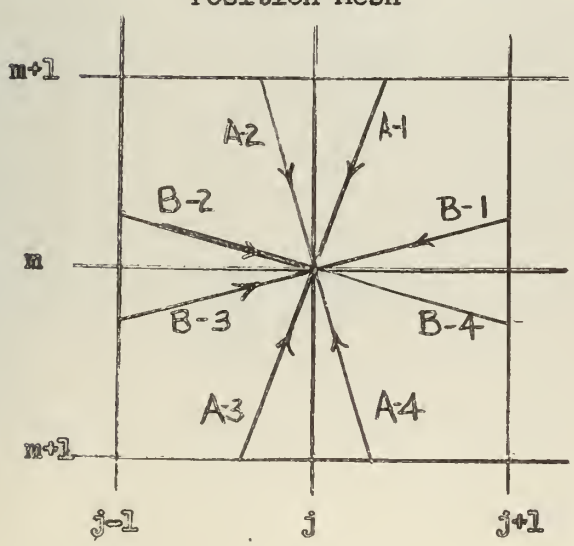

Table I

In all A cases $|b_i| < |h_f|$

In all B cases $|b_i| > |h_f|$

Subcase	b_i	h_f
A1, B1	-	-
A2, B2	+	-
A3, B3	+	+
A4, B4	-	+

Considering subcase A-3 and integrating equation 5 and knowing that

$$\int_{r_{j-1}}^{r_j} \ell\phi^{i,f}(r,z)\, dr = \frac{\Delta_j}{2}\left[\ell\phi^{i,f}_{j,m} + \ell\phi^{i,f}_{j-1,m} \right]$$

Figure IV

Position Mesh for Case A

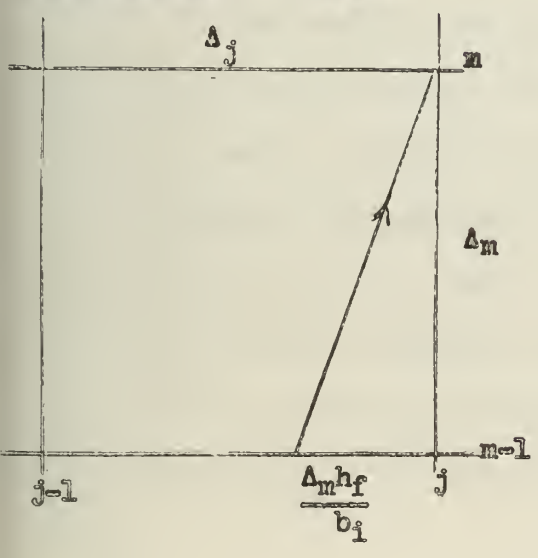

and

$$\int_{z_{m-1}}^{z_m} \ell\phi^{i,f}(r,z)\, dz = \frac{\Delta_m}{2}\left[\ell\phi^{i,f}_{j,m} + \ell\phi^{i,f}_{j,m-1} \right]$$

where $\Delta_j = r_j - r_{j-1}$ and $\Delta_m = z_m - z_{m-1}$

we obtain the following equation

$$\left|\frac{h_f}{\Delta_m}\right|\left[{}^{\ell}\phi^{i,f}_{j,m} + {}^{\ell}\phi^{i-1,f}_{j,m} - {}^{\ell}\phi^{i,f}_{j,m-1} - {}^{\ell}\phi^{i-1,f}_{j,m-1}\right] + \left|\frac{b_i}{\Delta_j}\right|\left[{}^{\ell}\phi^{i,f}_{j,m-1}\right.$$

$$\left. + {}^{\ell}\phi^{i-1,f}_{j,m-1} - {}^{\ell}\phi^{i,f}_{j-1,m-1} - {}^{\phi}\phi^{i-1,f}_{j-1,m-1}\right] = -\left[g_f \; {}^{\ell}\Sigma^{m-1}_{j-1}\right.$$

$$\left. + \frac{c_i}{\bar{r}_{j-1}}\right]\left[\frac{{}^{\ell}\phi^{i,f}_{j,m} + {}^{\ell}\phi^{i,f}_{j-1,m-1}}{2}\right] - \left[g_f \; {}^{\ell}\Sigma^{m-1}_{j-1} - \frac{c_i}{\bar{r}_{j-1}}\right]\left[\frac{{}^{\ell}\phi^{i-1,f}_{j,m} + {}^{\ell}\phi^{i-1,f}_{j-1,m-1}}{2}\right]$$

$$+ \frac{1}{\Delta_j}\left[\frac{b_i - d_i}{2}\right]\left[{}^{\ell}\phi^{i-1,f}_{j,m} + {}^{\ell}\phi^{i-1,f}_{j,m-1} - {}^{\ell}\phi^{i-1,f}_{j-1,m} - {}^{\ell}\phi^{i-1,f}_{j-1,m-1}\right]$$

$$+ \frac{e_i g_f}{2}\left[{}^{\ell}S_{j,m} + {}^{\ell}S_{j-1,m-1}\right] \qquad (18)$$

Where Σ^{m-1}_{j-1} is the total cross section of the material at the center of the grid in figure 4, i.e., the material to the left and below the j,m point and $\bar{r}_{j-1}$ is $\frac{r_j + r_{j-1}}{2}$.

The radial direction of integration is determined by the sign of η, i.e., by the sign of the b_i or d_i. Consequently, the signs of η, b_i, d_i, and Δ_j all change together. Likewise, the direction of integration axially is determined by the sign of μ, i.e., by the sign of h_f. Consequently the signs of μ, h_f and Δ_m all change together. If we use absolute magnitude signs for these quantities all Case A equations will be identical insofar as the signs of various terms are concerned. Similarly, all Case B equations will be identical.

If we now add the following expression to both sides of equation (18)

$$\left|\frac{b_i}{\Delta_j}\right|\left[{}_{\ell}\phi^{i,f}_{j-1,m-1} + {}_{\ell}\phi^{i-1,f}_{j-1,m-1} - {}_{\ell}\phi^{i,f}_{j,m} - {}_{\ell}\phi^{i-1,f}_{j,m}\right],$$

we obtain

$$\left[\left|\frac{h_f}{\Delta_m}\right| - \left|\frac{b_i}{\Delta_j}\right|\right]\left[{}_{\ell}\phi^{i,f}_{j,m} + {}_{\ell}\phi^{i-1,f}_{j-1,m-1} - {}_{\ell}\phi^{i,f}_{j,m-1} - {}_{\ell}\phi^{i-1,f}_{j,m-1}\right] =$$

$$-\left[g_f\,{}_{\ell}\Sigma^{m-1}_{j-1} + \frac{c_i}{\bar{r}_{j-1}}\right]\left[\frac{{}_{\ell}\phi^{i,f}_{j,m} + {}_{\ell}\phi^{i,f}_{j-1,m-1}}{2}\right] - \left[g_f\,{}_{\ell}\Sigma^{m-1}_{j-1}\right. \tag{18a}$$

$$\left. + \frac{c_i}{\bar{r}_{j-1}}\right]\left[\frac{{}_{\ell}\phi^{i-1,f}_{j,m} + {}_{\ell}\phi^{i-1,f}_{j-1,m-1}}{2}\right] + \left[\frac{|b_i| - |d_i|}{2|\Delta_j|}\right]\left[{}_{\ell}\phi^{i-1,f}_{j,m} + {}_{\ell}\phi^{i-1,f}_{j,m-1}\right.$$

$$\left. - {}_{\ell}\phi^{i-1,f}_{j-1,m} - {}_{\ell}\phi^{i-1,f}_{j-1,m-1}\right] + \frac{e_i\,g_f}{2}\left[{}_{\ell}\bar{s}_{j,m} + {}_{\ell}s_{j-1,m-1}\right]$$

$$+ \left|\frac{b_i}{\Delta_j}\right|\left[{}_{\ell}\phi^{i,f}_{j-1,m-1} + {}_{\ell}\phi^{i-1,f}_{j-1,m-1} - {}_{\ell}\phi^{i,f}_{j,m} - {}_{\ell}\phi^{i-1,f}_{j,m}\right].$$

If this expression is multiplied by $|\Delta_j|\,\omega^{i,f}$ where $|\Delta_j|\,\omega^{i,f} = \left|\frac{b_i}{h_f}\right|\,|\Delta_m|$

we obtain

$$|b_i|\,(1-\omega^{i,f})\left[{}_{\ell}\phi^{i,f}_{j,m} + {}_{\ell}\phi^{i-1,f}_{j,m} - {}_{\ell}\phi^{i,f}_{j,m-1} - {}_{\ell}\phi^{i-1,f}_{j,m-1}\right] =$$

$$\omega^{i,f}\left[|b_i| + \frac{|\Delta_j|}{2}\left(g_f\,{}_{\ell}\Sigma^{m-1}_{j-1} + \frac{c_i}{\bar{r}_{j-1}}\right)\right]{}_{\ell}\phi^{i,f}_{j,m} + A_3\,\omega^{i,f}. \tag{18b}$$

Where

$$A_3 = \left[|b_i| - \frac{|\Delta_j|}{2} \left(g_f \, {}^{\ell}\Sigma_{j-1}^{m-1} + \frac{c_i}{r_{j-1}} \right) \right] \phi^{i,f}_{j-1,m-1}$$

$$- \left[|b_i| + \frac{|\Delta_j|}{2} \left(g_f \, {}^{\ell}\Sigma_{j-1}^{m-1} - \frac{c_i}{r_{j-1}} \right) \right] {}^{\ell}\phi^{i-1,f}_{j,m}$$

$$+ \left[|b_i| - \frac{|\Delta_j|}{2} \left(g_f \, {}^{\ell}\Sigma_{j-1}^{m-1} - \frac{c_i}{r_{j-1}} \right) \right] {}^{\ell}\phi^{i-1,f}_{j-1,m-1} + \frac{\epsilon_i g_f}{2} |\Delta_j| \left[{}^{\ell}\bar{S}_{j,m} + {}^{\ell}\bar{S}_{j-1,m-1} \right]$$

$$+ \left(\frac{|b_i| - |d_i|}{2} \right) \left[{}^{\ell}\phi^{i-1,f}_{j,m} + {}^{\ell}\phi^{i-1,f}_{j,m-1} - {}^{\ell}\phi^{i-1,f}_{j-1,m} - {}^{\ell}\phi^{i-1,f}_{j-1,m-1} \right] \qquad (18c)$$

And finally transposing terms in equation (18b) we obtain an expression for the vector flux at the point j,m.

$${}^{\ell}\phi^{i,f}_{j,m} = \frac{b_i \, (1-\omega^{i,f}) \left({}^{\ell}\phi^{i,f}_{j,m-1} + {}^{\ell}\phi^{i-1,f}_{j,m-1} - {}^{\ell}\phi^{i-1,f}_{j,m} \right) + \omega^{i,f} A_3}{|b_i| + \omega^{i,f} \frac{|\Delta_j|}{2} \left(g_f \, {}^{\ell}\Sigma_{j-1}^{m-1} + \frac{c_i}{r_{j-1}} \right)} \qquad (18d)$$

By use of similar procedures for developing the equations for the three remaining A subcases we obtain the three equations on the following pages.

For subcase A-4

$$\ell\phi^{i,f}_{j,m} = \frac{|b_i|\,(1-\omega^{i,f})\left(\ell\phi^{i,f}_{j,m-1} + \ell\phi^{i-1,f}_{j,m-1} - \ell\phi^{i-1,f}_{j,m}\right) + \omega^{i,f}A_4}{|b_i| + \omega^{i,f}\left|\frac{\Delta_j}{2}\right|\left(g_f\Sigma^{\ell m-1}_{j+1} + \frac{c_i}{\bar{r}_{j+1}}\right)} \qquad (19a)$$

where

$$A_4 = \left[|b_i| - \frac{|\Delta_j|}{2}\left(g_f\Sigma^{\ell m-1}_{j+1} + \frac{c_i}{\bar{r}_{j+1}}\right)\right]\ell\phi^{i,f}_{j+1,m-1}$$

$$-\left[|b_i| + \frac{|\Delta_j|}{2}\left(g_f\Sigma^{\ell m-1}_{j+1} - \frac{c_i}{\bar{r}_{j+1}}\right)\right]\ell\phi^{i-1,f}_{j,m}$$

$$+\left[|b_i| - \frac{|\Delta_j|}{2}\left(g_f\Sigma^{\ell m-1}_{j+1} - \frac{c_i}{\bar{r}_{m+1}}\right)\right]\ell\phi^{i-1,f}_{j+1,m-1}$$

$$+\frac{e_i g_f}{2}|\Delta_j|\left[\ell\bar{S}_{j,m} + \ell\bar{S}_{j+1,m-1}\right] + \left[\frac{|b_i| - |d_i|}{2}\right]\left[\ell\phi^{i-1,f}_{j,m} + \ell\phi^{i-1,f}_{j,m-1}\right.$$

$$\left. - \ell\phi^{i-1,f}_{j+1,m} - \ell\phi^{i-1,f}_{j+1,m-1}\right]. \qquad (19b)$$

For subcase A-1

$$\ell\phi^{i,f}_{j,m} = \frac{|b_i|(1-\omega^{i,f})\left(\ell\phi^{i,f}_{j,m+1} + \ell\phi^{i-1,f}_{j,m+1} - \ell\phi^{i-1,f}_{j,m}\right) + \omega^{if} A_1}{|b_i| + \omega^{if}\frac{|\Delta_j|}{2}\left(g_f \ell\Sigma^{m+1}_{j+1} + \frac{c_i}{\bar{r}_{j+1}}\right)} \qquad (20a)$$

where

$$A_1 = \left[|b_i| - \frac{|\Delta_j|}{2}\left(g_f \ell\Sigma^{m+1}_{j+1} + \frac{c_i}{\bar{r}_{j+1}}\right)\right]\ell\phi^{i,f}_{j+1,m+1}$$

$$-\left[|b_i| + \frac{|\Delta_j|}{2}\left(g_f \ell\Sigma^{m+1}_{j+1} - \frac{c_i}{\bar{r}_{j+1}}\right)\right]\ell\phi^{i-1,f}_{j,m}$$

$$+\left[|b_i| - \frac{|\Delta_j|}{2}\left(g_f \ell\Sigma^{m+1}_{j+1} - \frac{c_i}{\bar{r}_{j+1}}\right)\right]\ell\phi^{i-1,f}_{j+1,m+1} + \frac{e_i g_f}{2}\left[\ell S_{j,m} + \ell S_{j+1,m+1}\right]$$

$$+\left[\frac{|b_i| - |d_i|}{2}\right]\left(\ell\phi^{i-1,f}_{j,m} + \ell\phi^{i-1,f}_{j,m+1} - \ell\phi^{i-1,f}_{j+1,m} - \ell\phi^{i-1,f}_{j+1,m+1}\right) \qquad (20b)$$

For subcase A-2

$$\ell\phi^{i,f}_{j,m} = \frac{|b_i|(1-\omega^{i,f})\left(\ell\phi^{i,f}_{j,m+1} + \ell\phi^{i-1,f}_{j,m+1} - \ell\phi^{i-1,f}_{j,m}\right) + \omega^{i,f} A_2}{|b_i| + \omega^{i,f}\frac{|\Delta_j|}{2}\left(g_f \ell\Sigma^{m+1}_{j-1} + \frac{c_i}{\bar{r}_{j-1}}\right)} \qquad (21a)$$

where

$$A_2 = \left[|b_i| - \frac{|\Delta_j|}{2} \left({}_{g_f}\Sigma^{m+1}_{j-1} + \frac{c_i}{\bar{r}_{j-1}} \right) \right] {}_{\ell}\phi^{i,f}_{j-1,m+1}$$

$$- \left[|b_i| + \frac{|\Delta_j|}{2} \left({}_{g_f}\Sigma^{m+1}_{j-1} - \frac{c_i}{\bar{r}_{j-1}} \right) \right] {}_{\ell}\phi^{i-1,f}_{j,m}$$

$$+ \left[|b_i| - \frac{|\Delta_j|}{2} \left({}_{g_f}\Sigma^{m+1}_{j-1} - \frac{c_i}{\bar{r}_{j-1}} \right) \right] {}_{\ell}\phi^{i-1,f}_{j-1,m+1} + \frac{e_i g_f}{2} |\Delta_j| \left[{}_{\ell}S_{j,m} + {}_{\ell}S_{j-1,m+1} \right]$$

$$+ \left[\frac{|b_i| - |d_i|}{2} \right] \left[{}_{\ell}\phi^{i-1,f}_{j,m} + {}_{\ell}\phi^{i-1,f}_{j,m+1} - {}_{\ell}\phi^{i-1,f}_{j-1,m} - {}_{\ell}\phi^{i-1,f}_{j-1,m+1} \right] \qquad (21b)$$

A similar procedure is used in deriving the equations for the B cases; except that as shown in Figure 5 the r and z components of the flux are different because $b_i \neq h_f$. The method of deriving the flux equation for case B-3 is outlined on the following page. The equations for the other B cases are listed also.

Figure V

Position Mesh

Case B

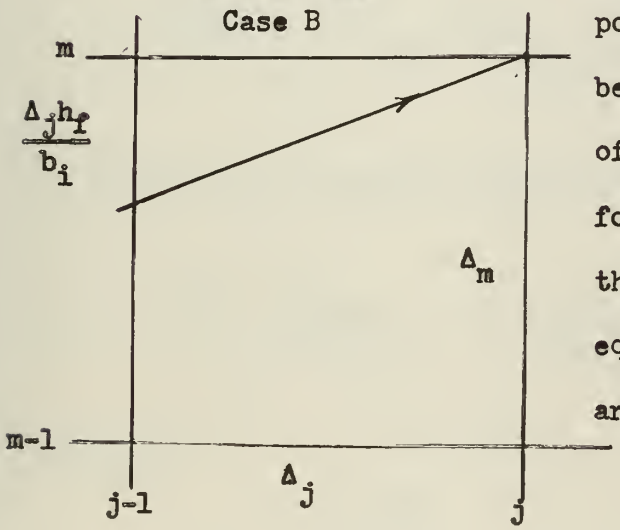

$$\left|\frac{h_f}{\Delta_m}\right|\left(\ell\phi^{i,f}_{j-1,m} + \ell\phi^{i-1,f}_{j-1,m} - \ell\phi^{i,f}_{j-1,m-1} - \ell\phi^{i-1,f}_{j-1,m-1}\right)$$

$$+\left|\frac{b_i}{\Delta_j}\right|\left(\ell\phi^{i,f}_{j,m} + \ell\phi^{i-1,f}_{j,m} - \ell\phi^{i,f}_{j-1,m} - \ell\phi^{i-1,f}_{j-1,m}\right) =$$

$$-\left[\underset{\sim}{g_f}\,\ell\Sigma^{m-1}_{j-1} + \frac{c_i}{\bar{r}_{j-1}}\right]\left[\frac{\ell\phi^{i,f}_{j,m} + \ell\phi^{i,f}_{j-1,m-1}}{2}\right]$$

$$-\left[\underset{\sim}{g_f}\,\ell\Sigma^{m-1}_{j-1} - \frac{c_i}{\bar{r}_{j-1}}\right]\left[\frac{\ell\phi^{i-1,f}_{j,m} + \ell\phi^{i-1,f}_{j-1,m-1}}{2}\right]$$

$$+\left[\frac{|b_i| - |d_i|}{2|\Delta_j|}\right]\left[\ell\phi^{i-1,f}_{j,m} + \ell\phi^{i-1,f}_{j,m-1} - \ell\phi^{i-1,f}_{j-1,m} - \ell\phi^{i-1,f}_{j-1,m-1}\right]$$

$$+\frac{e_i\,g_f}{2}\left[\underset{\sim}{\ell}\,S_{j,m} + \underset{\sim}{\ell}\,S_{j-1,m-1}\right] \qquad (22a)$$

To both sides of equation (22a) we add

$$\left|\frac{b_i}{\Delta_j}\right|\left(\ell\phi^{i,f}_{j-1,m-1} + \ell\phi^{i-1,f}_{j-1,m-1} - \ell\phi^{i,f}_{j,m} - \ell\phi^{i-1,f}_{j,m}\right.$$

and define

$$\omega^{\prime if} = \frac{|\Delta_j|}{|\Delta_m|}\left|\frac{h_f}{b_i}\right|$$

we obtain

$$\left|b_i\right|(1-\omega^{'if})\left[-\ell\phi^{i,f}_{j-1,m}-\ell\phi^{i-1,f}_{j-1,m}+\ell\phi^{i,f}_{j-1,m-1}+\ell\phi^{i-1,f}_{j-1,m-1}\right]=$$

$$-\left[\left|b_i\right|+\frac{\Delta_j}{2}\left(g_f\Sigma^{m-1}_{j-1}+\frac{c_i}{\bar{r}_{j-1}}\right)\right]\ell\phi^{i,f}_{j,m}+A_3 . \qquad (22b)$$

From this expression

$$\ell\phi^{i,f}_{j,m}=\frac{\left|b_i\right|(1-\omega^{'if})\left(\ell\phi^{i,f}_{j-1,m}+\ell\phi^{i-1,f}_{j-1,m}-\ell\phi^{i,f}_{j-1,m-1}-\ell\phi^{i-1,f}_{j-1,m-1}\right)+A_3}{\left|b_i\right|+\frac{\left|\Delta_j\right|}{2}\left(g_f\Sigma^{m-1}_{j-1}+\frac{c_i}{\bar{r}_{j-1}}\right)} \qquad (22c)$$

where A_3 is defined by equation (18c)

For case B-4

$$\ell\phi^{i,f}_{j,m}=\frac{\left|b_i\right|(1-\omega^{'if})\left[\ell\phi^{i,f}_{j+1,m}+\ell\phi^{i-1,f}_{j+1,m}-\ell\phi^{i,f}_{j+1,m-1}-\ell\phi^{i-1,f}_{j+1,m-1}\right]+A_4}{\left|b_i\right|+\frac{\left|\Delta_j\right|}{2}\left(g_f\Sigma^{m-1}_{j+1}+\frac{c_i}{\bar{r}_{j+1}}\right)} \qquad (23)$$

where A_4 is defined by equation (19b)

For case B-1

$$\ell\phi^{i,f}_{j,m}=\frac{\left|b_i\right|(1-\omega^{'i,f})\left[\ell\phi^{i,f}_{j+1,m}+\ell\phi^{i-1,f}_{j+1,m}-\ell\phi^{i,f}_{j+1,m+1}-\ell\phi^{i-1,f}_{j+1,m+1}\right]+A_1}{\left|b_i\right|+\frac{\left|\Delta_j\right|}{2}\left(g_f\Sigma^{m+1}_{j-1}+\frac{c_i}{\bar{r}_{j-1}}\right)} \qquad (24)$$

where A_2 is defined by equation (20b)

For case B-2

$$\ell\phi^{i,f}_{j,m} = \frac{|b_i|(1-\omega^{i,f})\left[\ell\phi^{i,f}_{j-1,m} + \ell\phi^{i-1,f}_{j-1,m} - \ell\phi^{i,f}_{j-1,m+1} - \ell\phi^{i-1,f}_{j-1,m-1}\right] + A_2}{|b_i| + \frac{|\Delta_j|}{2}\left(g_f \ell\Sigma^{m+1}_{j-1} + \frac{c_i}{\bar{r}_{j-1}}\right)} \qquad (25)$$

where A_2 is defined by equation (21b).

The vector fluxes defined by equations (18d), (19a), (20a), (21a), (22c), (23), (24), (25), are valid for all values of μ with the exceptions of the end points of our μ space where $\mu = \pm 1$. At these points trouble is experienced with singularities.[11] However, a modified equation may be derived by letting the terms containing $\frac{1}{r}$ in all equations following equation (1) be replaced by zero, since for $\mu = \pm 1$ the term in $\frac{1}{r}$ in equation (1) vanishes. This special equation was not needed since values of μ were chosen which avoided these singular points.

The procedures described above result in n equations. One more equation is needed and is provided by setting n = -1 in equation (3). The development above may be used when the values of b, c, ϕ_0, ϕ_{-1}, and ϵ used above are replaced by -1, 0, $\phi(\eta=-1)$, 0, and 1, respectively. These values reduce equation (6) to that found for the special case. Thus equation (6c) becomes with i = 0

$$\ell\phi^{0,f}_{j,m} = \frac{(1-\omega^{0,f})\ \ell\phi^{0,f}_{j,m-1} + \omega^{0,f} A_3}{1 + \frac{\omega^{0,f}|\Delta_j|}{2}\left(g_f \ell\Sigma^{m-1}_{j-1}\right)}$$

where

$$A_3' = \left[+1 - \frac{|\Delta_j|}{2} \left(g_f \ell \Sigma_{j-1}^{m-1} \right) \right] \ell \phi_{j-1,m-1}^{0,f} + \frac{g_f}{2} |\Delta_j| \left[\ell \bar{S}_{j,m} + \ell \bar{S}_{m-1,m-1} \right].$$

Nomenclature

b_i, c_i, d_i, e_i — Values obtained by differencing and integration of the transport equation over η, and defined by Equations 7a to 7d of Appendix A.

g_f, h_f — Values depending upon the quantized values of μ, and defined by Equations 7e and 7f of Appendix A.

$\hat{i}$ — a unit vector in the direction indicated by a subscript.

ℓ_p — Fraction of fission neutrons which are produced in a particular energy group ℓ.

r — The radial distance to a point.

$\bar{r}_h$ — The mean radius between two adjacent grid points.

z — The axial distance.

E — Neutron energy from a point. See Figure 1, Appendix A.

H_f — Values obtained by the use of the Gauss quadrature approximation to sum the flux over μ space, defined by Equation 13, Appendix A.

P_i — Values obtained by the use of the S_2 approximation to sum the flux over μ space, defined by Equation 12, Appendix A.

α — Ratio of the minimum neutron energy after scattering to its energy before scattering.

Δ Grid spacing of a mesh.

η Cosine of the angle ψ

θ Angle between the axis and the direction in which neutrons travel. See Figure I, Appendix A.

μ Cosine of the angle θ.

$\mu_{\ell k}$ The probability that a neutron which is scattered in the k^{th} group will land in the ℓ^{th} group.

ν Number of neutrons produced per fission.

Σ Total macroscopic cross section.

Σ_f Fission macroscopic cross section.

ℓ_γ^k The probability per unit length of neutron travel that a neutron is scattered in group k.

$\phi(r,z,\mu,\eta,v)$ Neutron flux which is classified according to speed, v, colatitude and azimuthal direction cosines μ and η, and position r and z.

ψ Colatitude angle denoting neutron travel with respect to the radius. See Figure I, Appendix A.

ω See defining equation Page A-12, Appendix A.

ω' See defining equation Page A-17, Appendix A.

$\hat{\Omega}$ Direction of unit vector in which neutrons travel.

Superscripts and Subscripts

i	Index labeling quantized values of η.
f	Index labeling quantized values of μ.
j	grid position index in the radial direction.
m	grid position index in the axial direction.
ℓ	neutron speed index.
k	neutron speed index of group in which neutron is scattered.

Appendix B

Whirlwind Program

Prior to the use of this program the following preset parameters must be defined and/or calculated:

pz1 = number of grid points in a radial direction less one

pz2 = number of grid points in an axial direction less one

pz3 = number of iterations, N, allowed at a set radius, in attempting to achieve a convergence of source pattern.

pz4 = number of adjustments, N', of radius allowed in attempting to achieve criticality.

pf2 $\geq$ drum address of cross section

pf1 + 92(pz1 + 2) (pz1 + 2)

pf3 = 92(pz2 + 2)

pf4 = 6(pz2 + 1)

The preset parameters listed below were used in the development of the program and have the values as indicated

pf1 = 5000; drum address of first flux at origin point.

pf5 = 704; address in fast memory at which the print-out routine will be placed when needed

pf10 = 2650; address of the print-out routine in the drum

pf15 = 300; length of the print-out routine

pf13 = 1470; address in the fast memory of the vector flux subroutine of the quadrant being calculated.

It is necessary also to furnish the program at

1) a9, the value of +(2pz1).0. This value is used in the calculation of $\frac{\Delta_j}{2}$

2) r4, the value of the first trial radius of core

3) r3, the value of the second trial radius of core

For a three group solution, values of each of the thirty-six fluxes and the three sources at each point are assumed and placed on tape in the order indicated in Table I.

Table I

Sequence of fluxes at a point

f	i	ℓ
0	0	0
		1
		2
	1	0
		1
		2
	2	0
		1
		2
1	0	0
•		
	•	
		•
$0 \leq f < 3$	$0 \leq i < 2$	$0 \leq \ell < 2$

The points are ordered as indicated in Table II.

Table II

Sequence of points

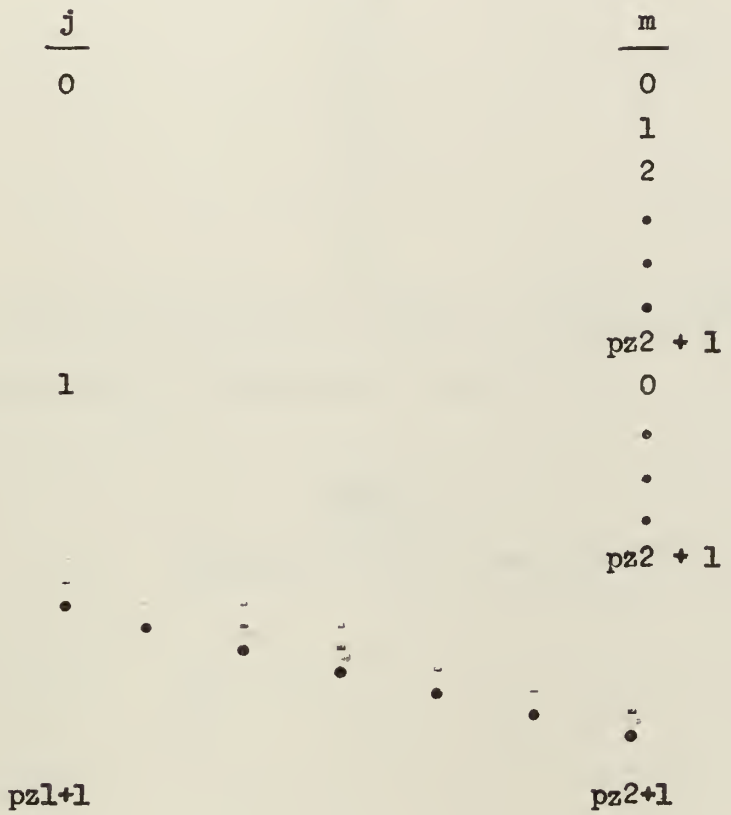

As explained in the Procedure the probability of scattering from group to group and fission cross section are associated with the grid points. These are also placed on the tape of data immediately following the flux for f = 3, i = 2, and ℓ = 2 in the order indicated on the following page in Table III.

Table III

Sequence of additional data for a point

γ^{11}

γ^{21}

γ^{31}

γ^{22}

γ^{32}

γ^{33}

Σf

The total scattering cross section is associated with the region between points and are ordered as in Table IV.

Table IV

Sequence of Total cross sections

j	m
0	0
	1
	.
	.
	.
	pz2
2	
.	
.	
.	
pz1	0
.	
.	
.	
	pz2

```
fc TAPE 410-316-1032 S2 AND GAUSS CAMPBELL AND PANCIERA
(24,6)
 pz1=5      pz2=5      pz3=20     pz4=20     pf1=5000   pf2=10000  pf3=644
 pf4=36     pf5=704    pf10=2650  pf13=1470  pf15=300
/Constants
 a1,+1.0    =0.333333  +0.6666667            a2,+0.0    +1.333333  +2.0
a3,+2.46    a4,-1.0    a5,+1.9677054         +1.1306938
+1.306938   +1.9677054           a6,+0.03     +0.03      +10.0      a7,+0.3183
+0.3634     +0.3183    a8,+0.6521452         +0.3478548             +0.3478548
+0.6521452  a9,+22.0    a10,+4.0   a11,+1.6944625       +0.3843341
/Cross Sections
 b1,+1.0    DITTO      12r/b2,+1.0           DITTO      12r/m6,+0  m7,+0
m8,pf3      m9,pf4     m10,+92    m11,+6     m12,pf1    m13,pf2    m14,+0
m15,+0
/RADII
r3,+0.0     r4,+0.0    r5,+0.0
/NORMALIZING CONSTANTS
d1,+0.0     d2,+0.0    d3,+0.0    r1,+0.0    r2,+0.0    s10,+0.0
/VARIABLES
 c1,+4.8    c2,=5.6    c3,+0.6885            +0.2295    +0.4590    +3.0355
+1.0118     +2.0236
/j-1,m-1 numbers
 n1,+1.0    DITTO      72r/s1,+1.0           +1.0       +1.0       t1,+1.0
+1.0        +1.0       +1.0       +1.0       +1.0       +1.0
/j-1,m numbers
n2,+1.0     DITTO      72r/s2,+1.0           +1.0       +1.0       t2,+1.0
+1.0        +1.0       +1.0       +1.0       +1.0       +1.0
/j-1,m+1, numbers
n3,+1.0     DITTO      72r/s3,+1.0           +1.0       +1.0       t3,+1.0
+1.0        +1.0       +1.0       +1.0       +1.0       +1.0
/j, m-1, numbers
n4,+1.0     DITTO      72r/s4,+1.0           +1.0       +1.0       t4,+1.0
+1.0        +1.0       +1.0       +1.0       +1.0       +1.0
/j,m numbers
n5,+1.0     DITTO      72r/s5,+1.0           +1.0       +1.0       t5,+1.0
+1.0        +1.0       +1.0       +1.0       +1.0       +1.0
/j,m+1, numbers
n6,+1.0     DITTO      72r/s6,+1.0           +1.0       +1.0       t6,+1.0
+1.0        +1.0       +1.0       +1.0       +1.0       +1.0
```

```
/j+1,m-1, numbers
n7,+1.0     DITTO    72r/s7,+1.0          +1.0     +1.0     t7,+1.0
+1.0        +1.0     +1.0       +1.0      +1.0     +1.0
/j+1.m, numbers
n8,+1.0     DITTO    72r/s8,+1.0          +1.0     +1.0     t8,+1.0
+1.0        +1.0     +1.0       +1.0      +1.0     +1.0
/j+1,m+1, numbers
n9,+1.0     DITTO    72r/s9,+1.0          +1.0     +1.0     t9,+1.0
+1.0        +1.0     +1.0       +1.0      +1.0     +1.0
/CONVERGED GAMMA
m1, itam18  itsr5    idva9      itsc1     isc0     icr3     isc1
icr6        isc2     icr2       m2,icac2  idvc1    isc2     idvall+c
isc0        imral+c  ics1       itsc3+c   isc0     ictm2    isc2
ictm2       isc0     icrpz3     m3,icaal  itss10   icac1    itsr1
isc1        icrpz1+1 isc2       icrpz2+1  m4,ispil isc2     ictm4
icar1       itsr2    iadc1      iadc1     itsr1    isc1     ictm4
isc0        ictm5    iSTOP      m5,icas10 icpm3    m18,ispo
/j,m SENSE AND CONTROL
i1,itai7    isc1     itim6      isc2      itim7    OUT      cam7
mhm10       s1h15    adm12      tsm15     cam8     mhm6     s1h15
tsm14       adm15    tsi6       cam15     sum10    tsm15    adm14
tsm29       cam14    sum8       adnk5     tsm26    cam14    adm8
adm15       tsm30    cam7       su1       mhm11    s1h15    adm13
tsm15       cam9     mhm6       s1h15     tsm14    adm15    tsm32
cam14       sum9     adm15      tsm31     cam6     dm0      cpi2
cam7        dm0      cpi3       IN        ispm23   ispm27   ispi5
i2,cam7     dm0      cpi4       IN        ispm23   ispm21   ispi5
i3,IN       ispm23   ispm24     ispi5     i4,IN    ispm23   ispm16
i5,iDOB     n5       i6,+0      +78       i7,ispo
/DATA READ IN PROGRAMME
m23,itam33  iDIB     n1         m26,+0    +276     iDIB     n4
m29,+o      +276     iDIB       n7        m30,+0   +276     iDIB
b1          m31,+0   +6         iDIB      b2       m32,+0   +6
m33,ispo
/ORIGIN PROGRAM
m16,itam17  ispp10   ispp13     icaal     idvt7    itsd1    ispe3
iDIB        pf13     +2050      +175      ispf1    m17,isp0
```

```
/CENTERLINE PROGRAM
m21,itam22  ispp4     isppl3    ispe3     iDIB      pf13      +2050
+175        ispf1     iDIB      pf13      +2475     +175      ispf18
m22,lsp0
/MIDPLANE PROGRAM
m24,itam25  ispp7     isppl3    ispe3     iDIB      pf13      +2050
+175        ispf1     iDIB      pf13      +2225     +125      ispf10
m25,ispQ
/GENERAL POINT PROGRAM
m27,itam28  isppl     isppl3    ispe3     iDIB      pf13      +2050
+175        ispf1     iDIB      pf13      +2225     +125      ispf10
iDIB        pf13      +2350     +125      ispf27    iDIB      pf13
+2475       +175      ispf18    m28,isp0
/Source S^c,S^1,S^2 at all Points
p13,itapl4  icat6     imrt5     itstl     icaa3     imrt5+12  imrt6+4
iadtl       itst7     icat6     imrt5+2   itstl     icat6+2   imrt5+6
iadtl       itst7+2   icat6     imrt5+4   itstl     icat6+2   imrt5+8
iadtl       itstl     icat6+4   imrt5+10  iadtl     itst7+4   pl4,isp0
/Source Normalization+Tolerance Program
e3,itae7    icat7+2   imrdl     itss5+2   icat7+4   imrdl     itss5+4
icat7       imrdl     itst7     isus5     icpe4     idvt7     isua6
icpe5       e6,icsa6  itssl0    ispe5     e4,idvt7  iada6     icpe6
e5,icat7    itss5     e7,isp0
/SCALAR Flux-General Point
pl,itap3    isc3      icr3      p2,icaa7  imrn5+c   itstl     icaa7+2
imrn5+6+c   iactl     itstl     icaa7+4   imrn5+12+c          iadtl
imra8       itstl     icaa7     imrn5+18+c          itst2     icaa7+2
imrn5+24+c  iadt2     itst2     icaa7+4   imrn5+30+c          iadt2
imra8+2     iadtl     itstl     icaa7     imrn5+36+c          itst2
icaa7+2     imrn5+42+c          iadt2     itst2     icaa7+4   imrn5+48+c
iadt2       imra8+4   iadtl     itstl     icaa7     imrn5+54+c
itst2       icaa7+2   imrn5+60+c          iact2     itst2     icaa7+4
imrn5+66+c  iadt2     imra6+6   iadtl     itst6+c   ictp2     p3,isp0
/Scalar Flux-Centerline Point
p4,itap6    isc3      icr3      p5,icaa8  imrn5+c   itstl     icaa8+2
imrn5+18+c  iadtl     itstl     icaa8+4   imrn5+36+c          iadtl
itstl       icaa8+6   imrn5+54+c          iadtl     imra7     itstl
icaa8       imrn5+6+c itst2     icaa8+2   imrn5+24+c          iadt2
```

```
itst2       icaa8+4   imrn5+42+c          iadt2     itst2     icaa8+6
imrn5+60+c  iadt2     imra7+2   iadtl     imra2+4   itst6+c   ictp5
p6,isp0
/Scalar Flux-Midplane Point
p7,itap9    isc3      icr3      p8,icaa7  imrn5+c   itstl     icaa7+2
imrn5+6+c   iadtl     itstl     icaa7+4   imrn5+12+c          iadtl
imra8       itstl     icaa7     imrn5+18+c          itst2     icaa7+2
imrn5+24+c  iadt2     itst2     icaa7+4   imrn5+30+c          iadt2
imra8+2     iadtl     imra2+4   itst6+c   ictp8     p9,isp0
Scalar Flux - Origin
p10,itap12  isc3      icr3      p11,icaa7 imrn5+c   itstl     icaa7+2
imrn5+6+c   iadtl     imra8     itstl     icaa7     imrn5+18+c
itst2       icaa7+2   imrn5+24+c          iadt2     imra8+2   iadtl
imra2+4     imra2+4   itst6+c   ictp11    p12,isp0
/RADIUS EXTRAPOLATION ROUTINE
qi,itaq9    icad2     isual     itstl     icpq2     q3,itst3  icad3
isual       itst2     icpq4     q5,itst4  isut3     icpq6     icad2
iexd3       itsd2     icar3     iexr4     itsr3     icat3     iext4
itst3       icatl     iext2     itstl     q6,icat3  isua6+2   icpq7
q8,icad2    isud3     itst6     icar4     isur3     imrtl     idvt6
iadr3       itsr3     q9,isp0   q2,imra4  ispq3     q4,imra4  ispq5
/Control
x1,icar4    isc4      icrpz4    ispm1     icad1     itsd3     x2,icar3
ispm1       icad1     itsd2     isc4      ictx3     iSTOP     x3,ispq1
ispx2       q7,iDIB   pf5       pf10      pf15      q10,isppf5
iSTOP
/WORKING FLUX
1470/y1,+0  DITTO     175r/y2,+0
/First Quadrant Flux
/First Flux
DA2050/ 1470/ f1,itaf3          isc3      icr3      f2,icsb2+6+c
imra5       imrc1     itstl     iada1     imrn9+c   itst2     icas5+c
iads9+c     imra5     imrc1     iadt2     imrc3     itst2     icstl
imrc3       iada1     itstl     icaa1     isuc3     imrn6+c   iadt2
idvt1       itsn5+c
/Second Flux
f4,icsa2+2  idvr1     itstl     icsb2+6+c imra5     itst2     iadtl
```

```
imrc1       itst3     iadal+2   imrn9+6+c itst4     icstl     iadt2
imrc1       itst6     iadal+2   imrn9+c   iadt4     itst4     icat6
isual+2     f5,imrn5+c          iadt4     itst4     icas5+c   iads9+c
imra5       imrc1     imra2+4   iadt4     itst4     icsal+4   iadal+2
idva2+4     itstl     ican6+c   iadn5+c   isun9+c   isun8+c   imrtl
iadt4       imrc3+2   itst4     f6,icst3  imrc3+2   iadal+2   itst2
icaal       isuc3+2   imral+2   itst3     ican6+6+c iadn6+c   isun5+c
imrt3       iadt4     idvt2     itsn5+6+c
/Third Flux
f7,icsb2+6+c          imra5+2   imrc1     itstl     iadal     imrn9+18+c
itst2       icas5+c   iads9+c   imra5+2   imrc1     iadt2     imrc3+6
itst2       icstl     iadal     imrc3+6   itstl     icac3+6   isual
itst3       ican8+18+c          isun9+18+c          imrt3     iadt2
idvtl       itsn5+18+c
/Fourth Flux
f8,icsa2+2  idvrl     itstl     icsb2+6+c imra5+2   itst2     iadtl
imrc1       itst3     iadal+2   imrn9+24+c          itst4     icstl
iadt2       imrc1     itst6     iadal+2   imrn9+18+c          iadt4
itst4       icat6     isual+2   imrn5+18+c          iadt4     itst4
f9,icas5+c  iads9+c   imra5+2   imrc1     imra2+4   iadt4     itst4
icsal+4     iadal+2   idva2+4   itstl     ican6+18+c          iadn5+18+c
isun9+18+c  isun 8+18+c         imrtl     iadt4     imrc3+8   itst4
icst3       imrc3+8   iadal+2   itst2     icaal     isuc3+8   imral+2
itst3       ican6+24+c          iadn6+18+c          isun5+18+c
imrt3       iadt4     idvt2     itsn5+24+c          ictf2     f3,isp0
/Second quadrant flux
/First flux
DA2225/ 1470/ f10,itaf17        isc3      icr3      f11,icsa2+2
idvr2       itstl     icsbl+6+c imra5     itst2     iadtl     imrc1
itst3       iadal+4   imrn3+12+c          itst4     icstl     iadt2
imrc1       itst6     iadal+4   imrn3+6+c iadt4     itst4     icat6
isual+4     imrn5+6+c f12,iadt4 itst4     icas5+c   iads3+c   imra5
imrc1       imra2+4   iadt4     itst4     icaal+4   isual+2   idva2+4
itstl       ican6+6+c iadn5+6+c isun3+6+c isun3+6+c itst3     ican6+12+c
iadn6+6+c   isun5+6+c imrt3     iadt4     idvt2     itsn5+12+c
/Second Flux
f14,icsa2+2 idvr2     itstl     icsbl+6+c imra5+2   itst2     iadtl
imrc1       itst3     iadal+4   imrn3+30+c          itst4     icstl
iadt2       imrc1     itst6     iadal+4   imrn3+24+c          iadt4
itst4       icat6     isual+4   imrn5+24+c          f15,iadt4 itst4
```

```
icas5+c     iads3+c     imra5+2     imrc1       imra2+4     iadt4       itst4
icaal+4     isual+2     idva2+4     itstl       ican6+24+c              iadn5+24+c
isun3+24+c  isun2+24+c              imrtl       iadt4       imrc3+10    itstl
icst3       iadal+4     imrc3+10    itst2       f16,icac3+10            isual
imral+4     itst3       ican2+30+c              iadn2+24+c              isun3+30+c
isun3+24+c  imrt3       iadtl       idvt2       itsn5+30+c              ictf11
f17,isp0
/Third Quadrant Flux
/First Flux
DA2350/ 1470/ f27, itaf33           isc3        icr3        f28,icsa2+2
idvr2       itstl       icsbl+c     imra5+4     itst2       iadtl       imrc1
itst3       iadal+4     imrnl+48+c              itst4       icstl       iadt2
imrc1       itstl       iadal+4     imrnl+42+c              iadt4       itst4
icatl       isual+4     imrn5+42+c              iadt4       itst4       f29,icas5+c
iadsl+c     imra5+4     imrc1       imra2+4     iadt4       itst4       icaal+4
isual+2     idva2+4     itstl       ican5+42+c              iadn4+42+c
isun2+42+c  isunl+42+c              imrtl       iadt4       imrc3+10    itstl
icst2       iadal+4     imrc3+10    itst2       icac3+10    isual       imral+4
itst3       ican2+48+c              iadn2+42+c              isunl+48+c
isunl+42+c  imrt3       iadtl       idvt2       f30,itsn5+48+c
/Second Flux
f31,icsa2+2 idvr2       itstl       icsbl+c     imra5+6     itst2       iadtl
imrc1       itst3       iadal+4     imrnl+66+c              itst4       icstl
iadt2       imrc1       itstl       iadal+4     imrnl+60+c              iadt4
itst4       icatl       isual+4     imrn5+60+c              iadt4       itst4
f32,icas5+c iadsl+c     imra5+6     imrc1       imra2+4     iadt4       itst4
icaal+4     isual+2     idva2+4     itst2       ican5+60+c              iadn4+60+c
isun2+60+c  isunl+60+c              imrt2       iadt4       imrc3+4     itstl
icst3       imrc3+4     iadal+4     itst2       icaal       isuc3+4     imral+4
itst3       ican4+66+c              iadn4+60+c              isun5+60+c
imrt3       iadtl       idvt2       itsn5+66+c              ictf28      f33,isp0
/Fourth Quadrant Flux
/First Flux
DA2475/ 1470/ f18, itaf26           isc3        icr3        f19,icsb2+c
imra5+4     imrc1       itstl       iadal       imrn7+36+c              itst2
icas5+c iads7+c         imra5+4     imrc1       iadt2       imrc3+6     itst2
icstl       iadal       imrc3+6     itstl       icac3+6     isual       itst3
ican8+36+c  isun7+36+c              imrt3       iadt2       idvtl       itsn5+36+c
```

```
/Second Flux
f20,icsa2+2 idvr1     itst1     icsb2+c   imra5+4   itst2     iadt1
imrc1       itst3     iadal+2   imrn7+42+c          itst4     icst1
iadt2       imrc1     itst6     iadal+2   imrn7+36+c          iadt4
itst4       icat6     isual+2   imrn5+36+c          iadt4     itst4
f21,icas5+c iads7+c   imra5+4   imrc1     imra2+4   iadt4     itst4
icaal+4     idva2+4   itst1     ican5+36+c          iadn4+36+c
isun8+36+c  isun7+36+c          imrt1     iadt4     imrc3+8   itst1
icst3       imrc3+8   iadal+2   itst2     f22,icaal isun3+8   imral+2
itst3       ican4+42+c          iadn4+36+c          isun5+36+c
imrt3       iadt1     idvt2     itsn5+42+c
/Third Flux
f23,icsb2+c imra5+6   imrc1     itst1     iadal     imrn7+54+c
itst2       icas5+c   iads7+c   imra5+6   imrc1     iadt2     imrc3
itst2       icst1     imrc3     iadal     itst1     icaal     isuc3
imrn4+54+c  iadt2     idvt1     itsn5+54+c
/Fourth Flux
f24,icsa2+2 idvr1     itst1     icsb2+c   imra5+6   itst2     iadt1
imrc1       itst3     iadal+2   imrn7+60+c          itst4     icst1
iadt2       imrc1     itst1     iadal+2   imrn7+54+c          iadt4
itst4       icat1     isual+2   imrn5+54+c          iadt4     itst4
f25,icas5+c iads7+c   imra5+6   imrc1     imra2+4   iadt4     icaal+2
isual+4     idva2+4   itst1     ican5+54+c          iadn4+54+c
isun8+54+c  isun7+54+c          imrt1     iadt4     imrc3+2   itst1
icst3       imrc3+2   iadal+2   itst2     icaal     isuc3+2   imral+2
itst3       ican4+60+c          iadn4+54+c          isun5+54+c
imrt3       iadt1     idvt2     itsn5+60+c          ictf19    f26,isp0
DA2650/ 704/ z1,itaz14          iscl      i crpz1+2 isc2      icrpz2+2
icadl       isp136z13 iscl      z12,itim6 isc2      z11,itim7 OUT
cam7        mhm10     slh15     adm12     tsm15     cam8      mhm6
slh15       adm15     tsz2      cam6      dm0       cpz3      cam7
dm0         cpz4      IN        ispz5     ispp1     ispz6     z3,cam7
dm0         cpz7      IN        ispz5     ispp4     ispz6     z4,IN
ispz5       ispp7     ispz6     z7,IN     ispz5     ispp10    ispz6
isc2        ictz11    iscl      ictz12    z14,isp0  z5,itaz8  iDIB
n5          z2,+0     +72       z8,isp0   z6,ispz6+1          z14,ispo
z10,icat6   isp139z13 icat6+2   isp139z13 icat6+4   isp136z13 z9,ispz7+4
z13.
```

Appendix C

Bibliography

BIBLIOGRAPHY

1. Trilling, C. A., "Organic Moderated Reactor Experiments", Nucleonics, Vol. 14, No.8.

2. Dowtherm Booklet, Dow Chemical Company, Midland, Michigan.

3. Gurinsky, D. H. and Dienes, G. J., Nuclear Fuels, D. Van Nostrand Co., Inc., Princeton, N.J., 1956

4. Freund, G. A., "Organic Coolant-Moderator for Power Reactors", Nucleonics, Vol 14, No. 8

5. Harvey, J. A. and Hughes, D. J., Neutron Cross Section, BNL 325 (1955).

6. Carlson, B. G., "Solution of the Transport Equation by S_n Approximation", LA-1891 (1955)

7. Clark, M. Jr., "S_n Method", N-22 Notes on Nuclear Reactor Theory for Spring 1956, Mass. Institute of Technology, 11 May 1956.

8. Hobson, E. W., The Theory of Spherical and Ellipsoidal Harmonics, Chapters 1, 2, Cambridge University Press, London, 1931.

9. Glasstone, S. and Edlund, M. C., The Elements of Nuclear Reactor Theory, D. Van Nostrand Co, Princeton, N. J., 1952.

10. Clark, M. L. Jr., N-22 Notes on Nuclear Reactor Theory for Spring 1956, problem 74, Mass. Institute of Technology.

11. Carlson, B. G., The "SNG Code". Los Alamos Scientific Laboratory of the University of California, Feb. 6, 1956.

12. Comprehensive Systems Manual, Mass. Institute of Technology Computer Laboratory, 1957.

JA 17 58
7 Sept. 59
BINDERY
INTERLIB
AEC

Thesis
C194 Campbell
35734
Whirlwind programming of S_2 approximation for flux distribution in a finite cylindrical reactor
JA 17 58
7 Sept. 59
BINDERY
INTERLIB
AEC

Thesis
C194 Campbell
35734
Whirlwind programming of S_2 approximation for flux distribution in a finite cylindrical reactor.

thesC194
Whirlwind programming of S(2) approximat
3 2768 002 08481 6
DUDLEY KNOX LIBRARY